



Article

Olive Anthracnose in Portugal Is Still Mostly Caused by *Colletotrichum nymphaeae*, but *C. acutatum* Is Spreading and *C. alienum* and *C. cigarro* Are Reported for the First Time

Ana Cabral ¹, Teresa Nascimento ¹, Helena G. Azinheira ^{1,2}, Andreia Loureiro ¹, Pedro Talhinhos ^{1,*} and Helena Oliveira ^{1,*}

¹ LEAF—Linking Landscape, Environment, Agriculture and Food Research Center, Associate Laboratory TERRA, Instituto Superior de Agronomia, Universidade de Lisboa, Tapada da Ajuda, 1349-017 Lisboa, Portugal; anacabral@isa.ulisboa.pt (A.C.); nascimento@isa.ulisboa.pt (T.N.); hmga@edu.ulisboa.pt (H.G.A.); andreialoureiro@isa.ulisboa.pt (A.L.)

² CIFC—Centro de Investigação das Ferrugens do Cafeeiro, Instituto Superior de Agronomia, Universidade de Lisboa; Tapada da Ajuda, 1349-017 Lisboa, Portugal

* Correspondence: ptalhinhos@isa.ulisboa.pt (P.T.); heloliveira@isa.ulisboa.pt (H.O.)

Abstract: Olive anthracnose, caused by *Colletotrichum* fungi, is responsible for major fruit yield losses and poor olive oil quality worldwide. In the Mediterranean basin, some *Colletotrichum* spp. appear to be replacing others, possibly due to climate change and modification in cultural systems. To update the situation in Portugal, 525 olive groves were surveyed throughout the country over two years, revealing a decrease in disease incidence, associated with scarcer rainfall and new cropping systems using less susceptible cultivars. A collection of 212 isolates was obtained, and phylogenetic analyses using a multi-locus sequencing approach (five and six loci in the *acutatum* and *gloeosporioides* species complex, respectively) revealed the presence of seven *Colletotrichum* species within the collection. Compared to surveys conducted in the first decade of the 21st century, the species composition of olive anthracnose pathogens in Portugal remains mostly unchanged, with *C. nymphaeae* as the prevalent species, followed by *C. godetiae*, but with *C. acutatum* geographically expanding and with *C. alienum* and *C. cigarro* being reported for the first time as causal agents of olive anthracnose in Portugal. A close attention to pathogen population shifts, in the context of climate change and modification of cultivation systems, is fundamental for anticipating plant protection measures.

Keywords: *Olea europaea*; *Colletotrichum* spp.; diversity; morphological analysis; phylogenetic analysis; pathogenicity



Citation: Cabral, A.; Nascimento, T.; Azinheira, H.G.; Loureiro, A.; Talhinhos, P.; Oliveira, H. Olive Anthracnose in Portugal Is Still Mostly Caused by *Colletotrichum nymphaeae*, but *C. acutatum* Is Spreading and *C. alienum* and *C. cigarro* Are Reported for the First Time. *Horticulturae* **2024**, *10*, 434. <https://doi.org/10.3390/horticulturae10050434>

Academic Editor: Harald Scherm

Received: 28 March 2024

Revised: 19 April 2024

Accepted: 22 April 2024

Published: 24 April 2024



Copyright: © 2024 by the authors. Licensee MDPI, Basel, Switzerland. This article is an open access article distributed under the terms and conditions of the Creative Commons Attribution (CC BY) license (<https://creativecommons.org/licenses/by/4.0/>).

1. Introduction

Olive (*Olea europaea* L. subsp. *europaea*) is the largest permanent crop worldwide accounting for 25% of the permanent crops in the world. Europe is the main continent where olives (65.7%) and olive oil (73.1%) are produced worldwide [1], with production concentrated mainly in the European Mediterranean countries. Olive trees are an integral part of the Portuguese landscape and olive oil is present in nearly all traditional cuisines. Despite being a small country, Portugal is in the top 10 of olive (ninth) and olive oil (eighth) producing countries, with olive groves being the largest agricultural crops in the country (379,565 ha) [2].

One of the fungal diseases that affects olive production and olive oil quality most worldwide is anthracnose, caused by several species of *Colletotrichum* [3–5]. On fruit, the disease appears during olive ripening, usually after the onset of autumn rains. The characteristic symptoms consist of sunken brown to black lesions on the fruit, which in moist conditions ooze mucilaginous masses of pink to orange conidia that emerge from acervuli. As the disease progresses, the infected fruits rot, resulting in fruit drop or mummification.

Defoliation and dieback of branches can also occur in severe epidemics, causing polyetic effects on the yield in subsequent years. Olive oils obtained from *Colletotrichum*-infected fruit present chemical and sensory defects that may prevent their direct use as virgin oils or result in a downgrading of the oil category, with severe economic losses for the olive grower [5,6]. These negative effects on olive oil were shown to be dependent on the *Colletotrichum* species–cultivar interaction [5].

Colletotrichum species responsible for olive anthracnose are remarkably diverse, and can be grouped into the acutatum, boninense and gloeosporioides species complexes [7–9] with a wide range of relative population frequencies [10–13]. Presently, at least 18 species of *Colletotrichum* are described as affecting olive trees worldwide: *C. acutatum*, *C. fiorinae*, *C. godetiae*, *C. lupini*, *C. nymphaeae*, *C. rhombiforme* and *C. simmondsii* (acutatum complex); *C. boninense* and *C. karsti* (boninense complex); and *C. aenigma*, *C. alienum*, *C. cigarro*, *C. fiorinae*, *C. fructicola*, *C. gloeosporioides*, *C. godetiae*, *C. perseae*, *C. queenslandicum*, *C. siamense* and *C. theobromicola* (gloeosporioides complex) [4].

Previous studies carried out in Portugal revealed that *C. nymphaeae* (formerly known as group A2 of *C. acutatum* [14]) was dominant, while *C. godetiae* (group A4 of *C. acutatum* [14]) was prevalent in the northeastern region (Trás-os-Montes), and these species, along with *C. acutatum* s.str. (group A5 of *C. acutatum* [9]) and *C. gloeosporioides* s.str., occurred at similar proportions in the southernmost region (Algarve) [10]. For this reason, the Algarve region was considered a hot spot of host–pathogen diversity in Portugal. Differences in *Colletotrichum* species virulence suggested that the most common population in Portugal (*C. nymphaeae*) was also the most virulent [11,12,14], with important olive cultivar × pathogen population interactions [15]. Information from other parts of the world reveals mixed scenarios [15], for example, in Spain where the dominant olive anthracnose pathogen is *C. godetiae* [4], or Italy where *C. godetiae* is replaced by *C. acutatum* in the south of the country [16]. Also, in Spain, recent studies show a tendency for *C. godetiae* to displace *C. nymphaeae* (without total exclusion) when both species are co-inoculated on olive fruit [17].

The last systematic survey for olive anthracnose in Portugal dates back to the last decade. Since then, olive farming has undergone a fast intensification process in Portugal, mainly in Alentejo (southern region), the most important olive and olive oil producing region of the country, where traditional rainfed plantations are being extensively replaced by intensive and super-intensive irrigated olive groves. As a result, traditional olive cultivars are being replaced by new ones which are more productive and better adapted to the new production systems. In addition, Portugal, as well as other Mediterranean regions, is experiencing the effects of climate change, primarily affecting the southern regions of Portugal. Although the effect of climate change on olive anthracnose is not fully addressed in the literature, the effect of environmental conditions on host–pathogen interaction is known, involving the modulation of plant resistance and of pathogen virulence mechanisms. On the pathogen side, environmental variables, such as temperature and water availability, influence many stages of plant infection (sporulation, pathogen growth, and expression of virulence genes) as well as dispersal and pathogen overwintering [18]. It is reported that higher winter temperatures may be associated with severe olive anthracnose outbreaks in southern Italy due to continued infections of the pathogen [19]. Also, as a result of warming temperatures, it is expected that strains of pathogens better adapted to these conditions will emerge [18], which in the case of olive anthracnose could also be reflected in shifts in pathogen populations. Therefore, this new framework fully justifies the need to update previous data and verify whether the populations of *Colletotrichum* fungi have changed, as reported for other countries [13,20–23]. Thus, the objectives of this study were (i) to analyze the incidence and severity of olive anthracnose in the main growing regions of Portugal and to compare them to those obtained in the first decade of the century; and (ii) to perform genotypic and phenotypic characterization of *Colletotrichum* isolates associated with olive anthracnose in order to identify possible shifts in species composition and population frequency.

2. Materials and Methods

2.1. Disease Survey and Fungal Isolation

To investigate the population structure of the olive anthracnose pathogens, surveys were conducted during autumn of 2018 and 2019 in different districts of Portugal (Figures 1 and 2), at the fruit maturation stage. In total, 525 sites were surveyed (286 during 2018; 239 during 2019) and, for each collection site, the presence/absence of anthracnose symptoms and signs on fruit was recorded. In each site surveyed (i.e., in each olive grove), at least five randomly selected olive trees were sampled and at least 30 fruits were collected by randomly selecting these from the sampled trees. Further, the asymptomatic presence of inoculum was assessed by incubating symptomless fruit in a wet chamber (100% relative humidity, 22 °C) aiming to induce the development of acervuli.

The pathogen was isolated from fruit with typical anthracnose lesions by scraping the acervular conidial masses onto Petri dishes containing potato dextrose agar (PDA, BD-Difco, Sparks, MD, USA) amended with a bacterial growth inhibitor (chloramphenicol 250 µg/mL), and incubated for 7 days at 25 °C, in darkness. Single-spore cultures were obtained on PDA and used to perform further experiments.

2.2. Molecular Characterization

From the surveys, a collection of 212 *Colletotrichum* spp. isolates was established. Total genomic DNA was extracted from mycelium scraped from the PDA plates according to the protocol previously described [24]. DNA concentration measurements were conducted on Microplate Reader Biotek Synergy HT (BioTek Instruments, Winooski, VT, USA) and diluted to 10 ng/µL.

2.2.1. ISSR Analysis

Inter-Simple Sequence Repeat analysis was performed using the primers (AG)₈YT (Y = C + T) [25] and (CAG)₅ [26] to assess the genetic diversity of the 212 *Colletotrichum* isolates obtained. For comparative purposes, a collection of 19 isolates previously characterized as *C. acutatum* (three isolates), *C. fioriniae* (three isolates), *C. godetiae* (five isolates), *C. gloeosporioides* (two isolates), *C. nymphaeae* (five isolates), and *C. rhombiforme* (one isolate) was also included in this analysis (Table S1). PCR amplifications, cycle conditions, electrophoresis, and analyses of band patterns were conducted according to the methodology described previously [27]. The annealing temperature for the primer (CAG)₅ was 60 °C [28].

2.2.2. PCR Amplification and Sequencing

According to the ISSR analysis and based on cultural and morphological traits, a set of 47 isolates was established for multi-locus phylogenetic analyses. For the isolates that grouped in the *acutatum* species complex ($n = 36$), five loci, actin (ACT), β -tubulin 2 (TUB2), histone H3 (HIS3), nuclear ribosomal RNA-Internal Transcribed Spacer (ITS), and a 200-bp intron of glyceraldehyde-3-phosphate dehydrogenase (GAPDH), were amplified using, respectively, the primer pairs ACT-512F/ACT-783R [29] T1 [30]/Bt2B [31], CYLH3F/CYLH3R [32], V9G [33]/ITS4 [34], and GDF1/GDR1 [35]. For the isolates that were grouped in the *gloeosporioides* species complex ($n = 11$), six loci were used: ACT, TUB2, ITS, GAPDH, glutamine synthetase (GS), and an intergenic spacer between the 3' end of the *Apn2* gene and the mating type gene *mat1-2-1* (ApMAT) amplified with the primer pairs GSF1/GSR1 [36] and AMF1/AMR1, respectively [37]. PCR mixtures contained 1 × DreamTaq Buffer (Thermo Scientific, Vilnius, Lithuania) with 2 mM of MgCl₂, 0.24 µM of each primer, 32 µM of each dNTP, 0.6 units DreamTaq DNA polymerase, and 30 ng of genomic DNA or 3 µL of ultra-pure water PCR grade for the negative controls, in a final volume of 15 µL. For the amplification of TUB2, 5% of DMSO was also added to the PCR mixture. The amplifications were carried out in a S1000 Thermal Cycler (Bio-Rad, Hercules, CA, USA) and the cycle conditions were 94 °C for 5 min, followed by 40 cycles at 94 °C for 30 s, 52 °C for 30 s (ACT and HIS3), or 55 °C (ITS), or 56 °C (TUB2), or 58 °C (GS and GAPDH), or 60 °C (ApMAT), and 72 °C for 60 s, and a final elongation at 72 °C for

10 min. After confirmation by agarose gel electrophoresis, amplicons were sequenced by StabVida (Portugal). Sequences were assembled and edited to resolve ambiguities, using the SeqMan module of the Lasergene software package v5.05 (DNASTar, Madison, WI, USA). Consensus sequences for all isolates were compiled into a single file (Fasta format) and novel sequences were lodged in GenBank accession numbers PP506774-PP506995 and PP508293-PP508342.

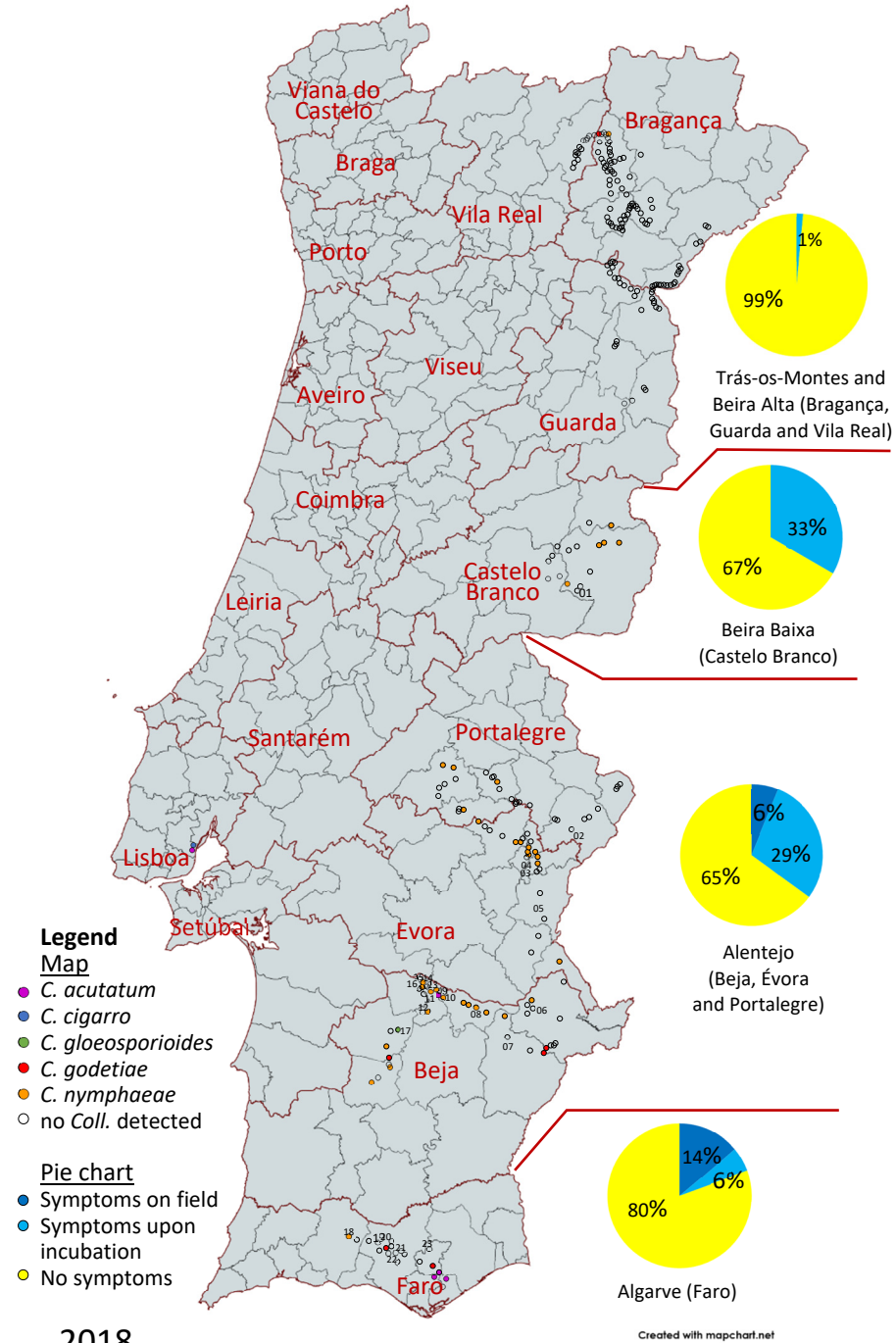


Figure 1. Survey of olive anthracnose in Portugal in 2018; pie charts represent the proportion of groves with symptoms in the field, symptoms upon incubation or no symptoms per region (*n* represents the number of olive groves surveyed); the map depicts the species of *Colletotrichum* (if any) identified in each location.

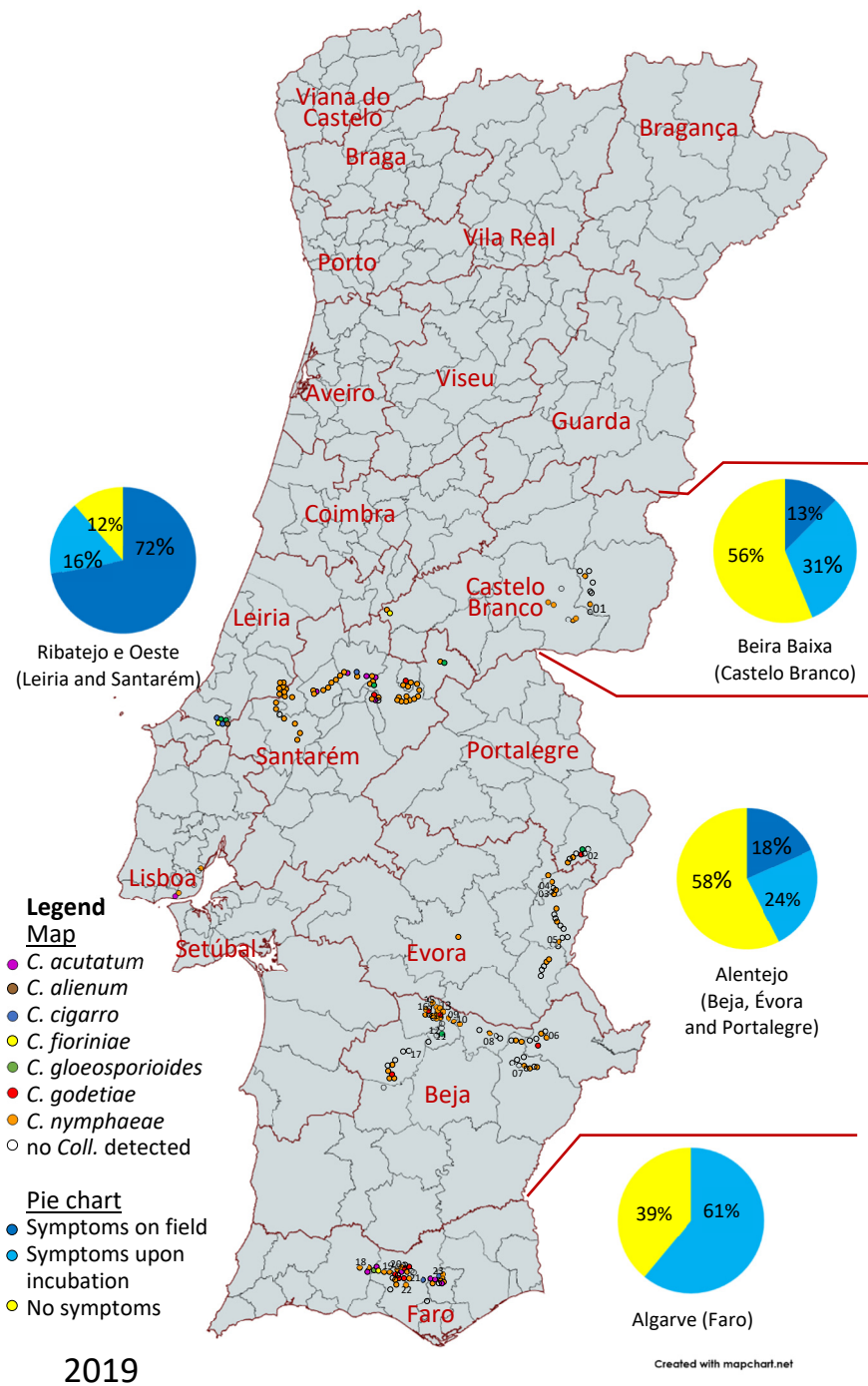


Figure 2. Survey of olive anthracnose in Portugal in 2019; pie charts represent the proportion of groves with symptoms in the field, symptoms upon incubation or no symptoms per region (n represents the number of olive groves surveyed); the map depicts the species of *Colletotrichum* (if any) identified in each location.

2.2.3. Phylogenetic Analyses

Colletotrichum sequences especially those representing the ex-type strains of the *acutatum* and *gloeosporioides* species complexes were obtained from GenBank and used as reference sequences (Table S2). Consensus sequences generated in this study and the reference sequences were aligned using MAFFT version 7 [38] and edited manually, if necessary, on MEGA 11 [39]. The alignments for each locus were combined in a single file using the program SEQUENCEMATRIX 1.8 [40]. The best-fit nucleotide substitution model for

each locus was calculated in MrModelTest v 2.4 [41], according to the Akaike information criterion. MrBAYES 3.2.7 [42] was used to perform the Bayesian analyses of the combined loci dataset incorporating the nucleotide substitution models selected by MrModelTest for each locus, which were GTR+G for ACT and HIS3, GTR+I for ITS, HKY+G for GAPDH, and TUB2, for the acutatum complex dataset; and GTR+G for GS and TUB2, GTR+I for ITS, HKY+G for ACT and ApMAT, and HKY+I for GAPDH, for the gloeosporioides complex dataset. The Markov Chain Monte Carlo sampling was set to 10 million generations, with two independent runs with four chains, and with the temperature set to 0.2. The tree samples of the two cold chains were compared every 1000 generations and stopped when the average standard deviation of split frequencies fell below 0.01. Burn-in was set at 25% after which the likelihood values were stationary, and the remaining trees were used to calculate posterior probabilities. Trees from different runs were then combined and summarized in a majority rule 50% consensus tree. Maximum likelihood (ML) was implemented in the CIPRES Science Gateway V 3.3 [43] using RAxML-HPC2 on XSEDE (8.2.12) using the GTRCAT model and 1000 rapid bootstrap inferences. The resulting trees were plotted using FigTree v. 1.4.4 (<http://tree.bio.ed.ac.uk/software/figtree>). Alignments and phylogenetic trees were lodged in TreeBASE (<http://www.treebase.org>; study number S31264).

2.3. Morphological Characterization

Colletotrichum isolates were inoculated on PDA and synthetic nutrient-poor agar (SNA, [44]) with two 1 cm² squares of filter paper on the agar surface. Cultures contained on PDA plates were incubated at 25 °C and, after 7 days of incubation, the colony diameter was measured and the cultural characteristics observed. Colony colors were rated according to the color chart of Rayner [45]. The SNA plates were incubated at 20 °C under white fluorescent light with a 12 h photoperiod. Morphological characters were examined using a Leica DM 2500 microscope with differential interference contrast illumination, and the images were captured with a Leica DFC295 digital camera using the software Leica Application Suite (LAS) version 3.3.0. Microscopic preparations were carried out in clear lactic acid. Conidial measures and descriptions were obtained from conidia that oozed from acervuli. Hyphal appressoria were observed on the reverse side of SNA plates. For each informative structure, 30 measurements were obtained. Measurements are presented as minimum–first quartile–third quartile–maximum.

Perithecia were induced in minimal salt medium agar with three autoclaved birch toothpicks in an “N” configuration on the medium surface to provide a substrate for the sexual structures [46]. The plates were incubated at 22 °C under white fluorescent light with a 12 h photoperiod, and the development of perithecia was examined up to 12 weeks after inoculation. Each experiment comprised three plates per isolate and was conducted twice.

2.4. Pathogenicity Assays

Olive fruit of the cultivar ‘Galega Vulgar’, at comparable ripening stages (3.3 to 3.5 according to [47]), were washed in water, surface-sterilized by being immersed in a 5% sodium hypochlorite solution (0.35% active chlorine) for 1 min, rinsed with sterile water, and dried on sterile tissue paper. *Colletotrichum* isolates of *C. acutatum* (19301A), *C. alienum* (19331), *C. cigarro* (18312B, 19148, 19151, 19300, 19329B, 19330A), *C. fioriniae* (19124A), *C. gloeosporioides* (19175), *C. godetiae* (19165), and *C. nymphaeae* (19112) were cultured on PDA at 25 °C for 7 days in the dark, prior to fruit inoculation. Nonwounded olives were inoculated by the deposition of a droplet (10 µL) of each conidial suspension (1×10^6 conidia mL⁻¹) onto the fruit epidermis. Negative controls were treated similarly, but the inoculum was replaced with 10 µL of sterile distilled water. Twelve replicates were used for each isolate. After inoculation, the fruits were maintained in a moist chamber at 22 °C in the dark over the first 24 h and then under a 12 h photoperiod and examined every 4–5 days. The experiments were conducted twice.

The disease severity on olive fruit was scored until 35 days after inoculation (dai) according to a 0–6 scale: 0, no symptoms; 1, mycelium only; 2, small necrosis (<5 mm

diameter), but no sporulation; 3, large necrosis (>5 mm diameter), but no sporulation; 4, few conidial masses on the inoculation point; 5, abundant conidial masses expanding away from the inoculation point; 6, conidial masses entirely covering the fruit [15]. A disease severity index (DSI) was calculated after 9, 15, and 35 dai using the following formula:

$$DSI (\%) = \frac{\sum(\text{class frequency} \times \text{score of rating class})}{\text{total number of fruit} \times \text{maximal disease index}} \times 100$$

The calculated DSI values were used to estimate the area under the disease progress curve (AUDPC) using the trapezoidal method [48] and the relative AUDPC (rAUDPC) was obtained by dividing each AUDPC by the highest theoretical AUDPC. One-way analysis of variance (ANOVA) was performed on rAUDPC as a function of the isolate, and the means were compared by Tukey's honestly significant difference (HSD) test with a level of significance of 0.05 using the software STATISTICA version 8.0 (StatSoft). To guarantee the homogeneity of variances, the 9 dai data were logarithmically transformed.

Re-isolations from the inoculated fruit were made onto PDA plates and the emergent colonies compared to the original isolates to fulfil Koch's postulates.

3. Results

3.1. Disease Survey

From the 286 different sites (olive groves) surveyed during autumn 2018 to investigate the presence of olive anthracnose, disease symptoms were observed in the field only at 11 sites (Figure 1). Symptoms were induced in samples from 38 sites after incubation of the symptomless fruits in a wet chamber, thus meaning that disease and/or inoculum were present in 17% of the sites and that in 83% of the sites no anthracnose was detected nor induced upon incubation. However, these proportions varied along the territory. Symptoms in the field were only detected in the south, in the Alentejo (Beja, Évora, and Portalegre districts) and Algarve (district of Faro) regions (in 6% and 14% of the sites surveyed, respectively), but the proportion of sites with anthracnose inoculum (symptoms in the field and symptoms upon incubation) was 35% in Alentejo, 33% in Beira Baixa (district of Castelo Branco), and 19% in Algarve. Whereas most sites in the Algarve where inoculum was detected also exhibited anthracnose symptoms, most sites with inoculum in Alentejo and Beira Baixa were asymptomatic in the field. At Trás-os-Montes and Beira Alta (districts of Bragança, Guarda, and Vila Real), anthracnose was only detected after fruit incubation, and only in two closely located sites. Therefore, no anthracnose disease was detected in 99% of sites in this region.

In 2019, symptoms were detected in the field in 29% of the sites surveyed and induced upon incubation in a wet chamber in another 29% of sites (Figure 2), meaning that anthracnose was not detected in 42% of sites (due to the sporadic detection of anthracnose in Trás-os-Montes and Beira Alta in 2018, these regions were not surveyed in 2019). These proportions varied over the country. No symptoms were detected in the field in Algarve, but 61% of the sites in this region revealed the presence of inoculum by inducing anthracnose symptoms upon incubation. At Alentejo, anthracnose was detected in 18% of sites, but anthracnose inoculum was present in 43% of sites. A similar situation could be depicted in Beira Baixa (13% and 44%, respectively). At Ribatejo e Oeste, however, anthracnose symptoms were detected in the field at 72% of the sites surveyed and another 16% of sites showed the presence of symptoms upon incubation, meaning that anthracnose inoculum remained undetected in only 11% of sites in this region.

Global disease incidence was higher in 2019 (29% olive groves exhibiting symptoms in the field) than in 2018 (4%). The asymptomatic presence of inoculum was also higher in 2019 (29% of samples) than in 2018 (13%). The analysis of accumulated rainfall from September to December, measured in a selection of meteorological stations from the Instituto Português do Mar e da Atmosfera (IPMA; www.ipma.pt; accessed on 6 July 2023) network, shows that both 2018 and 2019 had rainfall values below the 30-year normal curve for each station (Figure 3), with no notable differences between 2018 and 2019 that might explain

the differences in incidence. Rainfall in the previous months (January to August) was 147% in 2018 as compared to the average and 53% in 2019 (data from IPMA for the Faro, Beja, Castelo Branco, and Bragança weather stations), suggesting that the precipitation in that period also cannot explain the higher anthracnose incidence in 2019. Regarding temperature, the analysis of the anomaly in mean temperature values (<https://www.ipma.pt/pt/oclima/monitorizacao/>; accessed on 18 March 2024) countrywide reveals that late winter (February and March) was cooler than average in 2018 and mostly warmer than the average in 2019. In both years, a period of lower-than-average temperatures was recorded at the beginning of summer (in June in 2018 and in July in 2019), with the rest of the spring being similar to the average (except for May 2019, which was quite warmer). The two summers were distinct: mean temperatures were above average in 2018 and within average in 2019. In both autumns, mean temperatures fluctuated between values either slightly above or slightly below average.

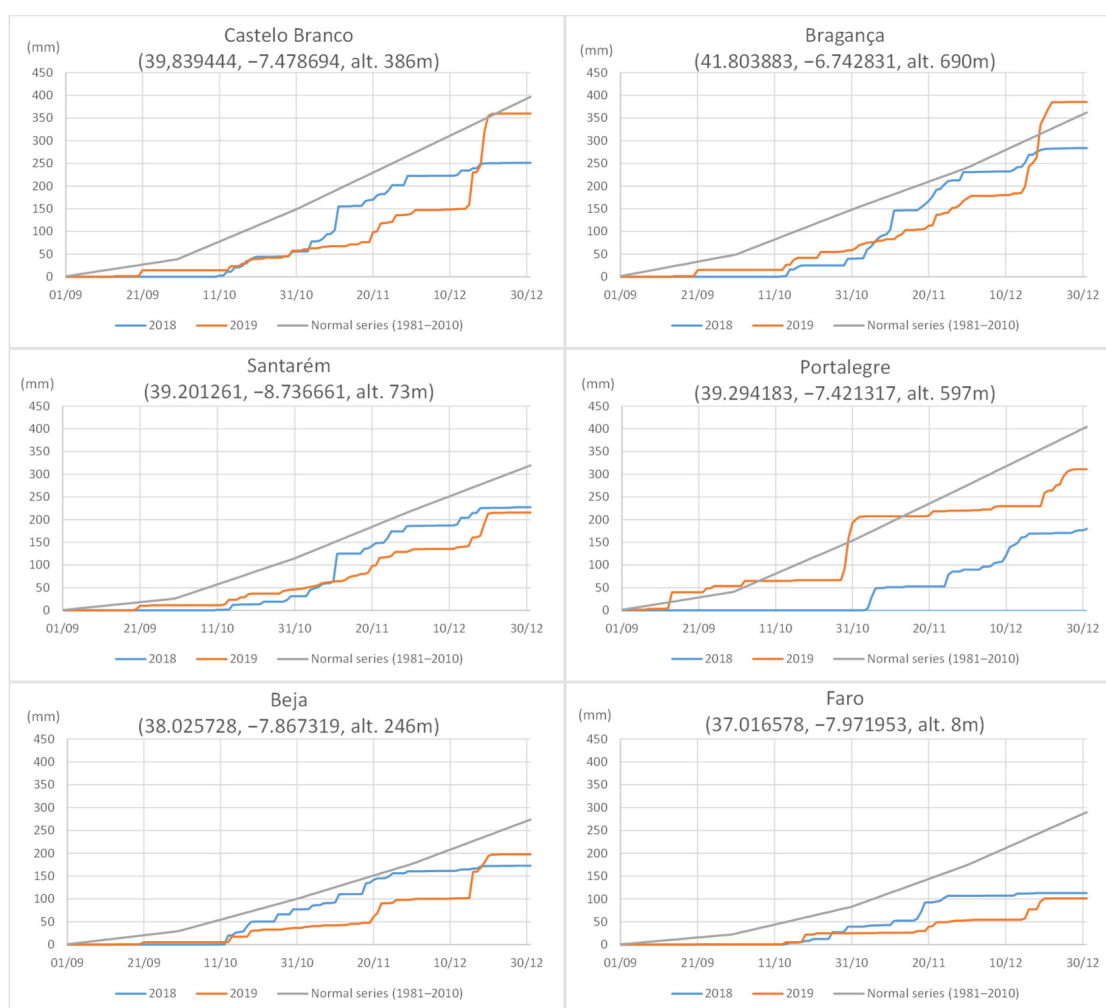


Figure 3. Accumulated rainfall in autumn 2018 and 2019 in Portugal (as measured at six meteorological stations) compared with 30-year normal curves; meteorological daily data and climatic normal retrieved from Instituto Português do Mar e da Atmosfera—IPMA; www.ipma.pt; accessed on 6 July 2023).

3.2. Molecular Characterization

3.2.1. ISSR Analysis

The ISSR primers produced multi-band patterns for each of the isolates present in the collection and for the 19 *Colletotrichum* isolates used as a reference for the species *C.*

acutatum, *C. fioriniae*, *C. gloeosporioides*, *C. godetiae*, *C. nymphaeae*, and *C. rhombiforme*. The primer (AG)₈YT generated 9 to 20 band fragments per isolate with an average of 16.4, and the primer (CAG)₅ generated 7 to 18 band fragments per isolate with an average of 11.1. Both primers were able to produce band patterns suitable to discriminate among the different species assigned to the reference isolates (Table S3).

A dendrogram was constructed, depicting similarity between the banding patterns of isolates (Figure S1). Most of the isolates ($n = 154$) clustered with the reference isolates of *C. nymphaeae* with a Dice similarity coefficient of 85.4% and a bootstrap (BS) of 100%, 19 isolates clustered along *C. acutatum* (similarity = 94%, BS = 100%), 19 isolates clustered with *C. godetiae* (similarity = 89.6%, BS = 100%), 8 isolates clustered along *C. gloeosporioides* (similarity = 87.2%, BS = 100%), and 4 with *C. fioriniae* (similarity = 82.2%, BS = 100%). Eight isolates did not group with any of the reference isolates used, although seven of them, 18312B, 19148, 19151, 19300, 19329B, 19330A, and 19342C, formed a well-defined cluster in the ISSR dendrogram with a similarity coefficient of 85% and a bootstrap value of 100%. Isolate 19331 did not group with any of the isolates tested. None of our isolates clustered with *C. rhombiforme*.

3.2.2. Phylogenetic Analyses

Acutatum Species Complex

The 36 isolates assigned to species in the acutatum complex according to ISSR analysis (i.e., *C. acutatum*, *C. fioriniae*, *C. godetiae*, and *C. nymphaeae*) were subjected to phylogenetic analysis using a five-locus concatenated dataset (ACT, TUB2, HIS, ITS, and GAPDH). Sequences from 129 strains representing 39 species of the acutatum species complex were retrieved from GenBank along with two representatives of *C. orchidophilum* (CBS 631.80 and CBS 632.80), used as outgroups, and added to the analysis creating a final dataset with 167 strains (Table S2).

The alignment comprised 1805 characters [ACT: 1–202; GAPDH: 203–460; HIS3: 461–832; ITS: 833–1324; TUB2: 1325–1805], including gaps, of which 1310 characters were constant, 177 characters were parsimony-uninformative, and 378 characters were parsimony-informative. The Bayesian analysis of the combined alignment resulted in a total of 151,082 trees of which 113,312 were sampled to calculate the majority-rule consensus tree and posterior probabilities, with a log likelihood value of -8263.03 . The best scoring RAxML tree had a final likelihood value of -7995.807650 .

The topologies obtained by the Bayesian consensus tree and ML analysis were identical in the five-locus concatenated data, and therefore only Bayesian consensus trees are presented with bootstrap support values (BS > 50%) and posterior probability values (PP > 0.90) near each node (Figure 4).

Twenty-one isolates clustered in a clade (BS = 88; PP = 0.99) that comprises several isolates of *C. nymphaeae*, including the ex-type strain of this species (CBS 515.78) but also the ex-type strains CBS 134233 of *C. citri* (regarded as a synonym of *C. nymphaeae*) and CGMCC3.16082 of *C. simulanticitri*. Twelve isolates (18105, 18123, 19112, 19182, 19213, 19262, 19281, 19285, 19290, 19291B, 19317, 19342A; group A) had the same nucleotide sequences in the five loci analyzed and were exactly equal to the isolates obtained from olives in Spain (Col-150) and Portugal (CBS 231.49, CBS 129945, Col-634, and PT800). The isolate 19190 also clustered with the isolates of group A, differing in TUB2 (1 bp). The isolate 18212 differed from the isolates of group A in TUB2 (1 bp) and in HIS3 (5 bp), and in the concatenated dendrogram it clustered with isolates obtained from strawberry in Canada, Israel, and Spain. The isolates 19125, 19131, 19149B, and 19154 (group B) clustered with isolate PT799 (from olives in Portugal) with a BS of 98% and a PP of 1 and differed from the isolates of group A in ITS (2 bp) and ACT (2 bp). The isolates 19122B, 19136, and 19153 (group C) clustered with isolate PT794 (from olives in Portugal) with a BS of 97% and a PP of 1. These isolates differed from the isolates of group A and B by 8 and 12 nucleotides, respectively, ITS (1 and 3 bp), ACT (1 and 3 bp), GAPDH (2 bp), and TUB2 (4 bp). Concerning the similarity to the ex-type strain CBS 515.78, 7 to 11 bp differences

were observed: ACT (1 and 2 bp in groups C and B, respectively), GAPDH (2 bp in groups A and B, 18212 and 19190), HIS3 (2 bp for groups A, B, C, and 19190, 7 bp for 18312), ITS (2 bp groups A, B, 18212 and 19190, 3 bp in group C) and in TUB2 (1 bp groups A, B, C, and 2 bp in 19190).

Eight isolates clustered in a clade (BS = 89; PP = 100) that comprised isolates identified as *C. godetiae* including the ex-type strain of this species. The isolates 18036, 18216, 19134, 19139, 19164A, and 19165 clustered (BS = 84; PP = 1) with isolates obtained from olives in Greece (CBS 193.32), Italy (CBS 130251), Spain (Col-50), and Portugal (PT797), and the sequences of these isolates were exactly identical to the ones of the isolates CBS 193.32 and CBS 130251. The isolates 19137 and 19293 differed in 2 bp and 3 bp, respectively, in ACT and in 1 bp in GAPDH from the other six isolates obtained, resulting in these isolates clustering apart. Concerning the similarity to the ex-type strain CBS 133.44, the eight isolates were identical in ITS and TUB2 and differed in ACT (3 bp for isolate 19293, 2 bp for isolate 19137, and 1 bp for the remaining isolates), GAPDH (1 bp for isolates 19137 and 19293, and 2 bp for the rest of the isolates), and HIS3 (2 bp).

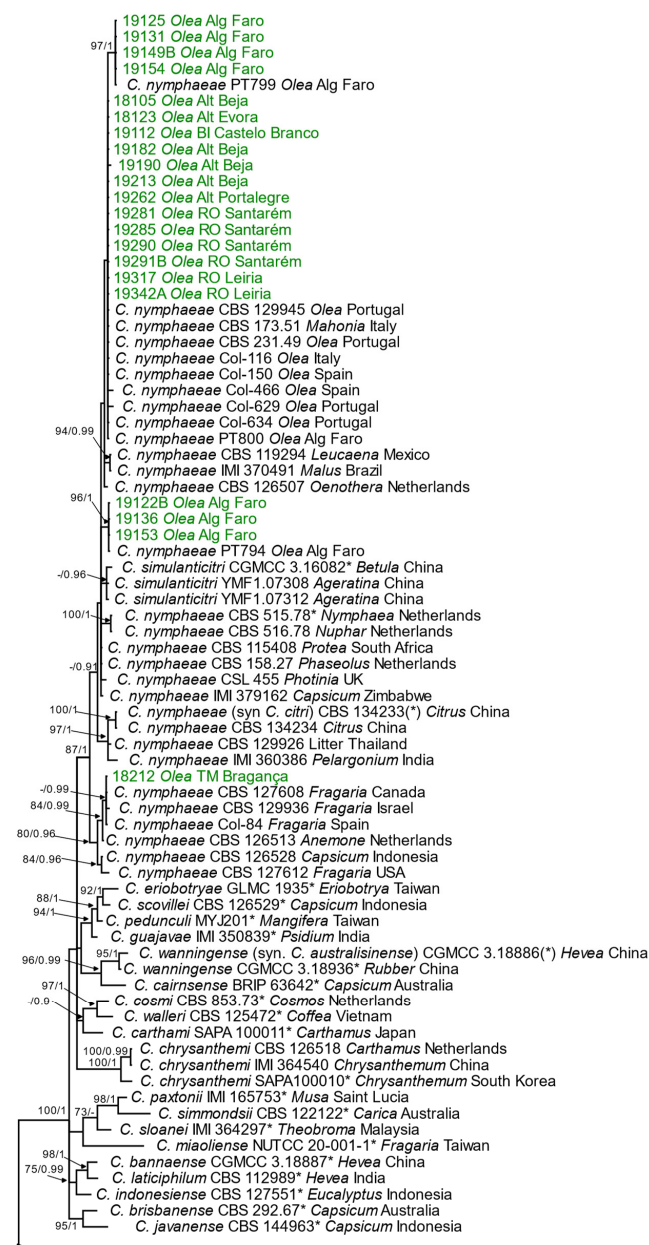


Figure 4. Cont.

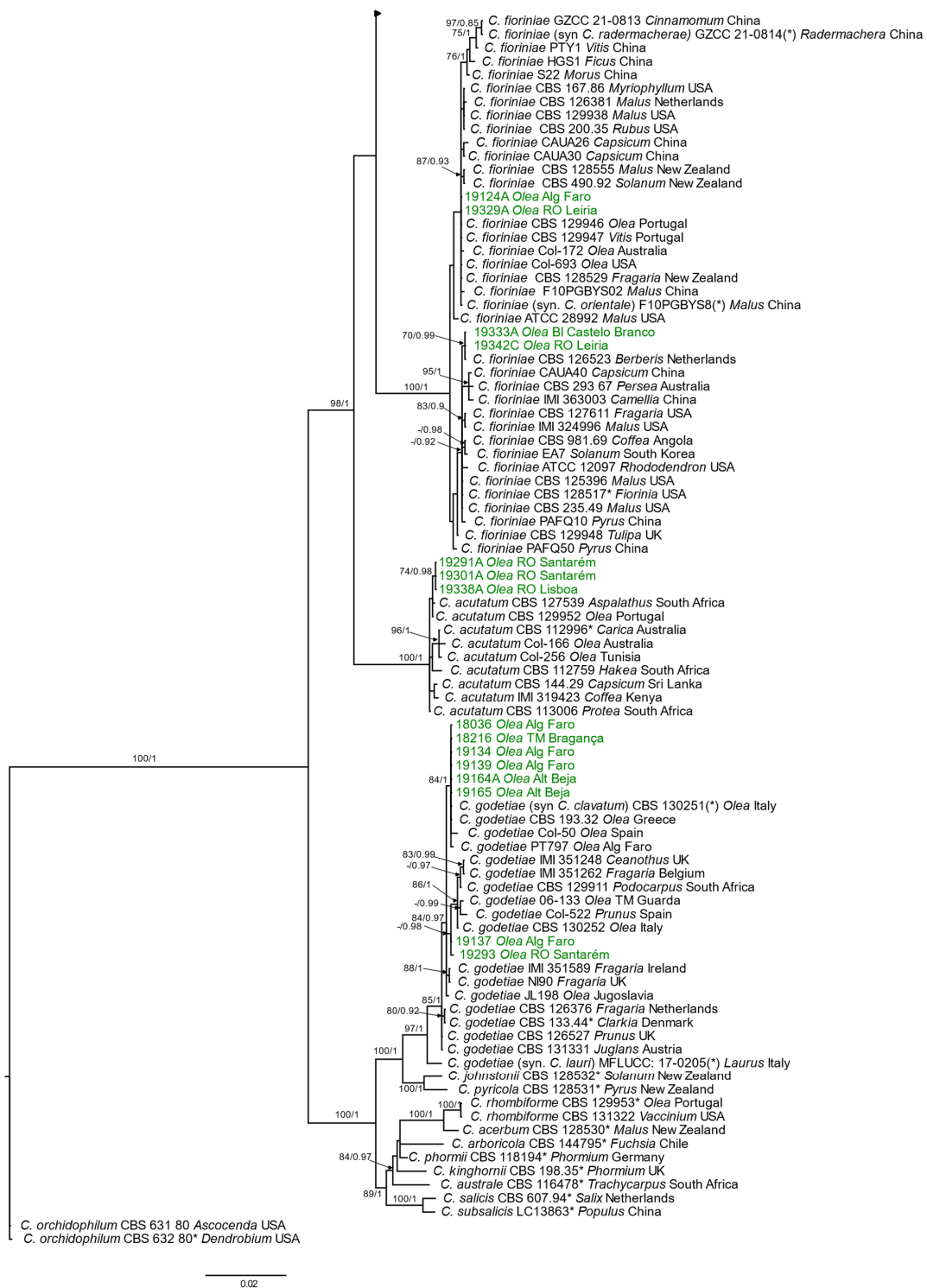


Figure 4. Fifty percent majority rule consensus tree from a Bayesian analysis based on a five-locus combined dataset (ACT, TUB2, HIS, ITS, and GAPDH) for *Colletotrichum* isolates of the acutatum complex. The RAxML bootstrap support values (BS, >70%) and Bayesian posterior probability (PP, >0.9) are displayed at the nodes (BS/PP). The tree was rooted with *C. orchidophilum* (CBS 631.80 and CBS 632.80). The scale bar indicates the expected substitutions per site. Isolates obtained in this study are indicated in green. Abbreviations: Alt—Alentejo, Alg—Algarve; BI—Beira Interior; RO—Ribatejo e Oeste; TM—Trás-os-Montes. Ex-type strains are emphasized with an asterisk* and the ex-type or authentic strain of synonymized taxon with (*).

Four isolates clustered in a clade (BS = 89; PP = 100) that comprised the ex-type strain of *C. fioriniae*, CBS 128517 and also the ex-type strains of *C. orientale* (F10PGBYS08) and *C. radermacherae* (GZCC 21-0814), synonyms of *C. fioriniae*. The isolates 19333A and 19342C differ from the ex-type strain of *C. fioriniae* (CBS 128517) only in 1 bp in ITS and the isolates 19124A and 19329A differ in 10 bp (1 bp in ACT, 2 bp in GAPDH, 4 bp in HIS3, and 2 bp in TUB2). The sequences of the isolates 19124A and 19329A were identical to the ones of isolates CBS 129946 (from olive in Portugal), CBS 129947 (from grapevine in Portugal), and CBS 128529 (from strawberry in New Zealand) and differed in 2 bp in TUB2 from isolate F10PGBYS08 (from apple in China).

The isolates 19291A, 19301A, and 19338A clustered in a clade (BS = 100; PP = 1) that encompassed *C. acutatum* isolates. These three isolates differed from isolate CBS 129952 (from olives in Portugal) in 1 bp in GAPDH, from CBS 127539 (from rooibos in South Africa) in 1 bp in GAPDH and TUB2, and from the ex-type strain of *C. acutatum* CBS 112996 (from papaya in Australia) in 5 bp in GAPDH and 1 bp in TUB2.

Gloeosporioides Species Complex

For the 11 isolates initially assigned to the gloeosporioides complex by ISSR analysis and/or morphological characterization (which includes the eight isolates that were not assigned to a species by ISSR), the phylogenetic analysis was performed using a six-locus concatenated dataset (ACT, GAPDH, GS, ITS, ApMAT, TUB2). The complete dataset consisted of sequences from 106 strains, including 43 ex-type strains and two *C. boninense* isolates (CBS 123755 and LF644) used as outgroups (Table S2). The alignment comprised 3249 characters [ACT: 1–237; GAPDH: 238–470; GS: 471–1384; ITS: 1385–1854; ApMAT: 1855–2614; TUB2: 2615–3249] including gaps, of which 1794 characters were constant, 626 characters were parsimony-uninformative, and 829 characters were parsimony-informative. Also, for each locus, individual trees were obtained. The Bayesian analysis of the combined alignment resulted in a total of 129,002 trees of which 96,752 were sampled to calculate the majority-rule consensus tree and posterior probabilities, with a log likelihood value of $-16,215.55$. The best scoring RAxML tree had a final likelihood value of $-16,128.251903$.

The topologies obtained by the Bayesian consensus tree and ML analysis were identical in the six locus-concatenated data and therefore only Bayesian consensus trees are presented with bootstrap support values (BS > 50%) and posterior probability values (PP > 0.90) near each node (Figure 5).

One isolate (19331) was identified as *C. alienum* as the nucleotide sequences of ACT, GAPDH, GS, ITS, and TUB2 were similar to the ones of the ex-type strain ICMP 12071 (from apple in New Zealand). A 1-bp difference in ApMAT was found for isolates obtained from olive in Australia (Col-211) and Uruguay (isolate OL98). No nucleotide sequence available in GenBank was 100% identical to that of the ApMAT fragment sequenced for isolate 19331, with all differences being 1 bp or more.

Seven isolates were identified as belonging to *C. cigarro*. These isolates differed from the ex-type strain of *C. cigarro* (ICMP 18539, from olive in Australia) in 1 to 3 bp (isolates 19148, 19151, 19300, 19329B and 19330A), in 9 bp (18312B), and in 13 bp (19342B). These differences were observed in ApMAT (1 bp: 18312B, 19148, 19151, 19300, 19329B; 19330A; 3 bp: 19342B), in GS (1 bp: 19300; 2 bp: 19151; 9 bp: 18312B and 19342B), GAPDH (2 bp: 19329B and 19330A), and in TUB2 (1 bp: 19342B). The isolates 18312B and 19342B cluster with isolates F317 and Isol.53 (from olive in Italy) from which they do not differ in GS, ITS, and TUB2 (except 19342B that differed in 1 bp). The isolates 19329B and 19330A were similar to isolate CVG628 (from blueberry in Italy; retrieved from GenBank as *C. helleniense*) in GAPDH but differed in 1 bp in ACT and GS and 2 bp in ApMAT. In our phylogenetic analysis, this isolate did not group with the ex-type strain of this species, CBS 142418, suggesting that this strain may rather belong to *C. cigarro*.

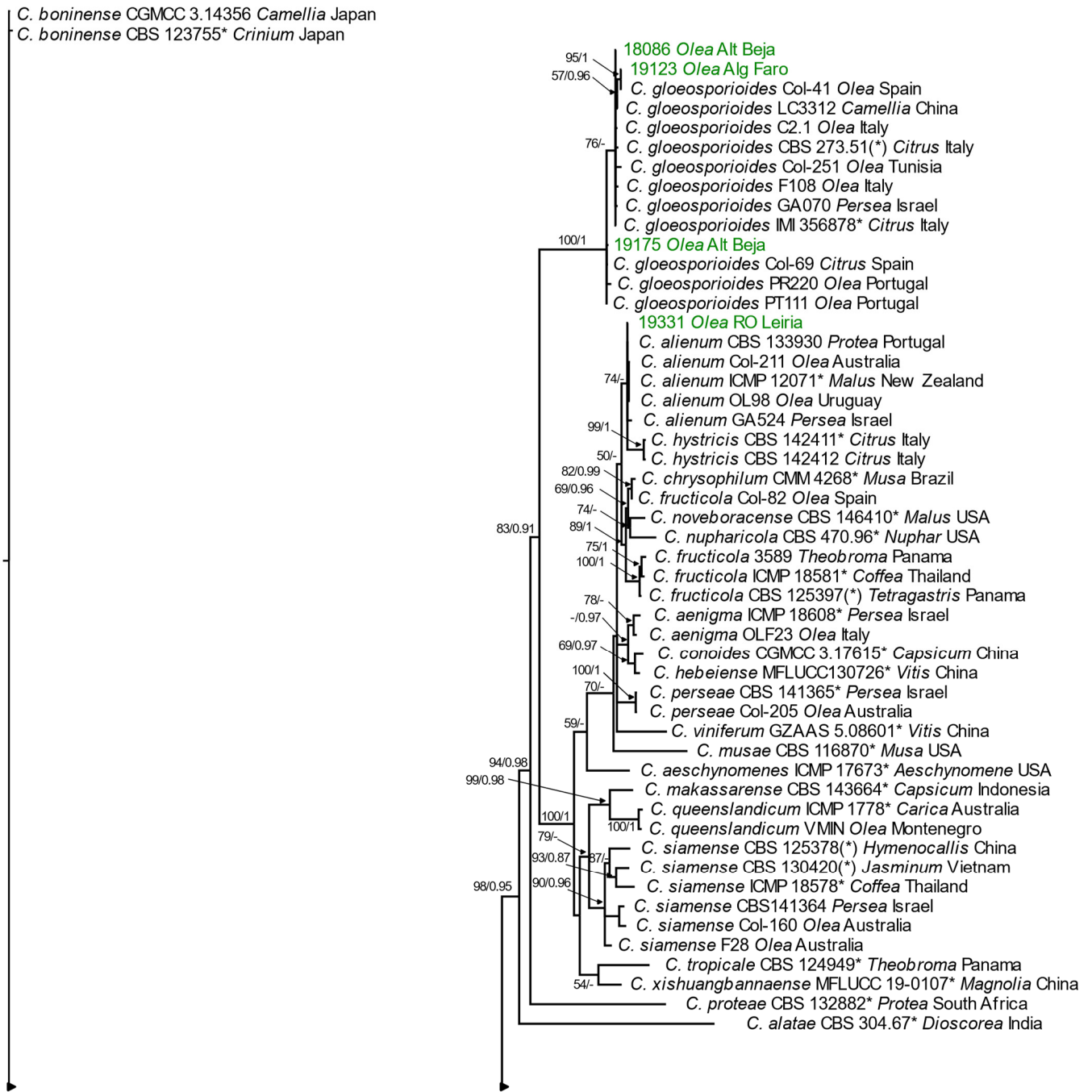


Figure 5. Cont.

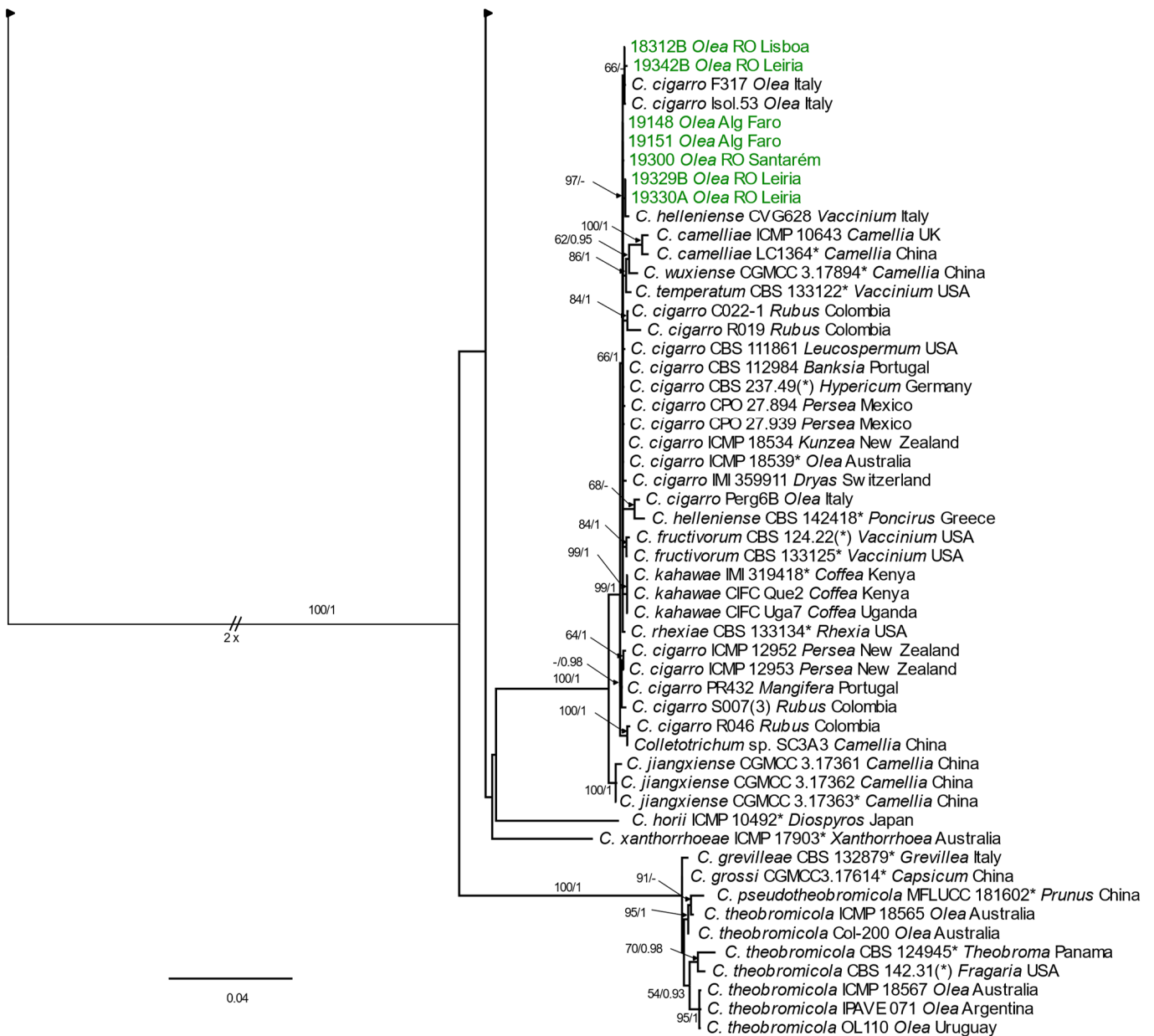


Figure 5. Fifty percent majority rule consensus tree from a Bayesian analysis based on a six-locus combined dataset (ACT, GAPDH, GS, ITS, ApMAT, and TUB2) for *Colletotrichum* isolates of the gloeosporioides complex. The RAxML bootstrap support values (BS, >70%) and Bayesian posterior probability (PP, >0.9) are displayed at the nodes (BS/PP). The tree was rooted with *C. boninense* (CBS 123,55 and LF644). The scale bar indicates the expected substitutions per site. Isolates obtained in this study are indicated in green. Abbreviations: Alt—Alentejo, Alg—Algarve; RO—Ribatejo e Oeste. Ex-type strains are emphasized with an asterisk* and the ex-type or authentic strains of synonymized taxon with (*).

Three isolates (18036, 19123, 19175) clustered into the *C. gloeosporioides* clade (BS = 100; PP = 1). The sequences of ApMAT, GAPDH, GS, ITS, and TUB2 were identical to the ones of the ex-type strain of *C. gloeosporioides* IMI 35678 (from orange in Italy) for isolate 18036, and differed in 4 nucleotides (1 in ITS and 3 in ApMAT) or in 18 nucleotides (5 in GAPDH, 12 in GS, and 1 in ITS) for isolates 19123 and 19175. The isolate 19123 was similar to isolate Col-41 from olives in Spain in ApMAT, GAPDH, ITS, and TUB2, and isolate 19175 was similar in ApMAT, GS, ITS, and TUB2 to isolate PT110 from olives in Portugal.

3.3. Morphological Characterization

Detailed morphological observations were conducted for the same 47 *Colletotrichum* isolates selected for phylogenetic analysis and assigned to seven *Colletotrichum* species, in which four species belonged to the acutatum complex and three to the gloeosporioides one. Among the latter, *C. alienum* and *C. cigarro* are reported for the first time in Portugal as causal agents of olive anthracnose. A morphological description of each species is provided below.

3.3.1. Acutatum Species Complex

Colletotrichum acutatum J.H. Simmonds, Queensland J. agric. Anim. Sci. 25: 178A. 1968 (Figure 6A–E).

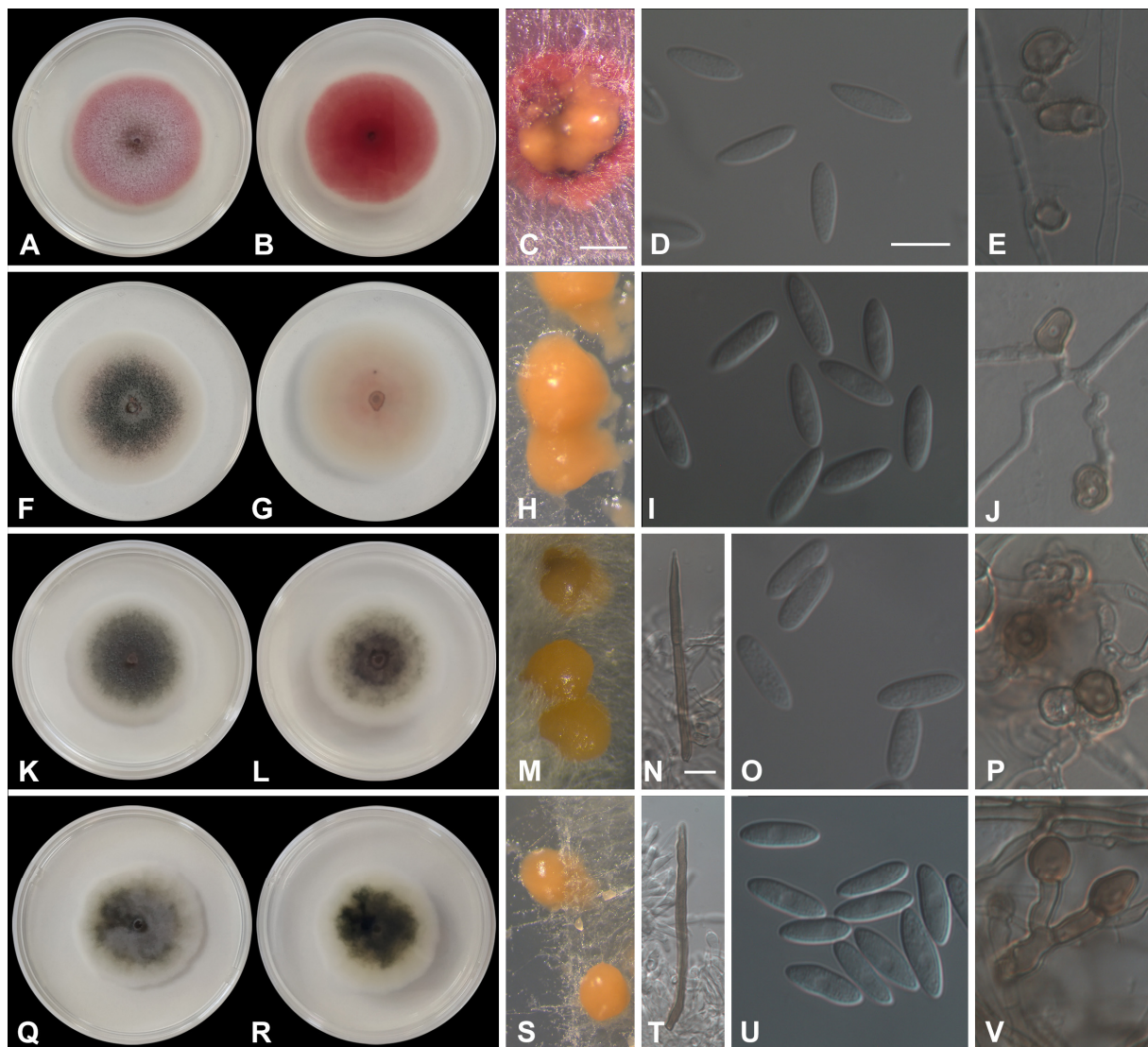


Figure 6. Morphological and cultural characters of *Colletotrichum* isolates from the acutatum complex: *C. acutatum* isolate 19301A (A–E); *C. fiorinae* isolate 19124B (F–J); *C. godetiae* isolate 19293 (K–P); *C. nymphaeae* isolates 19112 (Q–S,U,V) and 18212 (T). Colonies on PDA, upper (A,F,K,Q) and reverse (B,G,L,R) sides. Acervuli (C,H,M,S), seta (N,T), conidia (D,I,O,U) and appressoria (E,J,P,V) on SNA. Scale bars = 10 µm. Scale bar of (C) applies to (H,M,S), of (N) applies to (T), and of (D) applies to (E,I,J,O,P,U,V).

A sexual morph was not observed. An asexual morph was observed on synthetic nutrient agar (SNA). Acervuli peach formed on filter paper. Setae were not observed.

Conidia were hyaline, smooth-walled, aseptate, straight, cylindrical-to-fusiform with both ends acute, (7.3–)11.4–14.3(–16.5) × (2.7–)3.7–4.4(–5.3) µm mean ± SD = 12.6 ± 1.9 × 4 ± 0.5 µm. L/W ratio = 3.1. Appressoria were solitary, medium brown, smooth-walled, ellipsoidal-to-obovate, entire edge, and sometimes undulate, (5.3–)8.1–9.4(–13.4) × (4.8–)5.8–7.3(–8.4) µm, mean ± SD = 9 ± 1.8 × 6.4 ± 0.9 µm. L/W ratio = 1.4. Chlamydospores were not observed.

Culture characteristics: Colonies on potato dextrose agar (PDA) had a 56 to 60 mm diameter after 7 days at 25 °C, and were flat with an entire margin; their surface was rose to red with white margins, aerial mycelium was white to pale mouse gray, and reverse was red to rose with a white margin.

Colletotrichum fioriniae (Marcelino & Gouli) R.G. Shivas & Y.P. Tan, Fungal Diversity 39: 117. 2009 (Figure 6F–J).

A sexual morph not observed. An asexual morph was observed on SNA. Acervuli, which were salmon to orange, formed on filter paper. Setae were not observed. Conidia were hyaline, smooth-walled, aseptate, straight, and fusiform with both ends acute, (10.6–)12.2–13.8(–16.7) × (3.6–)4.2–4.7(–5.2) µm, mean ± SD = 13.1 ± 1.3 × 4.4 ± 0.3 µm. L/W ratio = 3. Appressoria were solitary or in loose groups, pale to medium brown, smooth-walled, ellipsoidal, clavate to irregular outline, entire edge or undulate, (6.9–)7.5–8.8(–14.1) × (5.2–)5.9–6.8(–7.6) µm, mean ± SD = 8.8 ± 2.1 × 6.3 ± 0.6 µm. L/W ratio = 1.4. Chlamydospores were not observed.

Culture characteristics: Colonies on PDA had a 51 to 60 mm diameter after 7 days at 25 °C, and were flat with an entire margin; their surface was purplish gray to white, pale purplish gray in the middle to grayish rose and a white margin, and reverse pale vinaceous to vinaceous buff to white, grayish rose with a white margin, and with conidial masses that were salmon to orange.

Colletotrichum godetiae Neerg., *Friesia* 4: 72. 1950 (Figure 6K–V).

A sexual morph was not observed. An asexual morph was observed on SNA. Acervuli luteus which were orange formed on filter paper. Setae present (isolates 19164A and 19293) were medium brown, smooth-walled, 1–2-septate, 45–75 µm long, and base-cylindrical, with a 4–5 µm diam, tip ± acute. Conidia were hyaline, smooth-walled, aseptate, straight, and cylindrical-to-clavate with one end round and the other slightly acute (8.6–)12.6–14.4(–18.6) × (3.2–)4.3–4.9(–5.9) µm, mean ± SD = 13.5 ± 1.5 × 4.6 ± 0.5 µm. L/W ratio = 3. Appressoria were solitary, medium-brown, smooth-walled, and clavate-to-elliptical, with the edge entire or undulate (6.6–)9.1–11.5(–14.4) × (3.9–)5–6.1(–7.8) µm, mean ± SD = 10.4 ± 1.9 × 5.5 ± 0.8 µm, L/W ratio = 1.9. Chlamydospores were not observed.

Culture characteristics: Colonies on PDA had a 43 to 54 mm diameter after 7 days at 25 °C, and were flat with an entire margin; surface olivaceous gray, with a vinaceous buff in the middle, to olivaceous gray with a white margin, with the reverse similar to surface.

Colletotrichum nymphaeae (Pass.) Aa, Netherlands J. Pl. Pathol., 84: 110 (1978) (Figure 6Q–V).

= *Colletotrichum simulanticitri* Z.F. Yu, Journal of Fungi 8 (2, no. 185): 24 (2022)

A sexual morph was not observed. An asexual morph was observed on SNA. Acervuli which were saffron to orange formed on filter paper. Setae were medium brown, with the basal cell sometimes pale brown, smooth-walled, 0–2-septate, 35–70 µm long, with the base cylindrical, 3–4 µm diam, tip ± acute observed only in the isolates 18212, 19122B, 19131, 19190, 19262, 19285, 19291B, and 19317. Conidia were hyaline, smooth-walled, aseptate, straight, cylindrical to cylindrical-clavate with one end round and the other end was round or slightly acute (8.4–)11.4–13.3(–16.8) × (2.8–)3.9–4.3(–5.3) µm, mean ± SD = 12.3 ± 1.5 × 4.1 ± 0.4 µm, L/W ratio = 3. Appressoria were solitary, medium-brown, smooth-walled, clavate-to-elliptical, or irregular in outline, entire, with an undulate to lobate margin (5.5–)7.8–10(–14.8) × (3.9–)5.9–7.1(–11.1) µm, mean ± SD = 9.2 ± 1.7 × 6.6 ± 1 µm. L/W ratio = 1.4. Chlamydospores were not observed.

Culture characteristics: Colonies on PDA had a 43 to 60 mm diameter after 7 days at 25 °C, and were flat with the entire margin. The surface mouse was gray to white, or

olivaceous gray with white margins, reverse white with grayish fructification, mouse gray, or olivaceous gray, with white margins.

Notes: *Colletotrichum simulanticitri* was described from a leaf spot of *Ageratina adenophora* and *Betula* sp. in China [49]. The three isolates from this study were included in our phylogeny and grouped in the *C. nymphaeae* clade. The ex-type strain of *C. simulanticitri* (YMF1.07302) and the ex-type strain of *C. nymphaeae* (CBS 515.78) have a sequence similarity of 99.59% in ACT (245/246 identities which includes one gap), 100% in CHS-1 (226/226), 99.19% in GAPDH (245/247), and 99.26% in ITS (538/542 which includes two gaps). On the other hand, isolates CBS 127608 and IMI 360386, identified as *C. nymphaeae* in a phylogenetic study with 70 isolates of this species [8], differ from the type strain in 6 or 11 nucleotides, respectively (0 or 3 in ACT, 2 or 1 in CHS-1, 2 or 5 in GAPDH, and 2 in ITS), thus presenting similar to or greater nucleotide differences than those observed in the isolate YMF1.07302 of *C. simulanticitri* to the ex-type strain of *C. nymphaeae*. Furthermore, the etymology of species epithet *simulanticitri* refers to the similarity of this species to *C. citri*, which was already regarded as a synonym of *C. nymphaeae* when this species was described [50].

3.3.2. Gloeosporioides Species Complex

Colletotrichum alienum B.S. Weir & P.R. Johnst., Stud. Mycol. 73: 139 (2012) (Figure 7A–H).

A sexual morph was observed on the toothpicks on minimal salt medium (MSM): Perithecia were pale brown to brown, and dark-walled globose to sub-globose, with a short ostiolar neck, often in clusters. Asci were eight-spored, $53\text{--}62 \times 9\text{--}13 \mu\text{m}$. Ascospores were hyaline, aseptate, smooth, cylindrical, curved, tapering slightly to each end ($14.5\text{--}15.5\text{--}17.2\text{--}18.3$) \times ($3.5\text{--}4.2\text{--}4.6\text{--}5.4$) μm , mean \pm SD = $16.3 \pm 1 \times 4.4 \pm 0.3 \mu\text{m}$, L/W ratio = 3.7. An asexual morph was observed on SNA. Setae were not observed. Conidia were cylindrical with broadly rounded ends ($13.4\text{--}14.7\text{--}16.1\text{--}17.9$) \times ($4.5\text{--}5\text{--}5.3\text{--}5.8$) μm , mean \pm SD = $15.4 \pm 1.2 \times 5.2 \pm 0.3 \mu\text{m}$, L/W ratio = 3. Appressoria were mostly simple, globose to cylindrical ($5.4\text{--}10\text{--}11.7\text{--}15.1$) \times ($4.9\text{--}5.8\text{--}7.9\text{--}8.9$) μm , mean \pm SD = $10.9 \pm 2.5 \times 6.9 \pm 1.2 \mu\text{m}$, L/W ratio = 1.6. Chlamydospores were not observed.

Culture characteristics: Colonies on PDA > 85 mm diameter after 7 days at 25 °C, flat with entire margin; aerial mycelium dense, cottony, pale gray in the middle to white, reverse dark gray in the middle with sporadic black flecks, pale gray to white towards the edge.

Colletotrichum cigarro (B.S. Weir & P.R. Johnst.) A. Cabral & P. Talhinhas, Plants (Basel) 9 (4): no. 502, 12 (2020) (Figure 7I–Q).

A sexual morph was observed on the toothpicks: Perithecia were pale brown to brown, dark-walled globose to sub-globose, with a short ostiolar neck, often in clusters. Asci were eight-spored, $55\text{--}75 \times 9\text{--}13 \mu\text{m}$. Ascospores were hyaline, aseptate, smooth, cylindrical, curved, tapering slightly to each end ($15.5\text{--}18.1\text{--}19.8\text{--}22.9$) \times ($3.8\text{--}4.3\text{--}5\text{--}5.7$) μm , mean \pm SD = $19 \pm 1.7 \times 4.6 \pm 0.5 \mu\text{m}$, L/W ratio = 4.1. An asexual morph was observed on SNA. Setae were not observed. Conidia were cylindrical with broadly rounded ends ($10.1\text{--}14.1\text{--}15.9\text{--}17.8$) \times ($3.1\text{--}4.5\text{--}5.4\text{--}6.3$) μm , mean \pm SD = $14.8 \pm 1.4 \times 4.9 \pm 0.7 \mu\text{m}$, L/W ratio = 3. Appressoria were simple, globose to fusiform, with the margin mostly lobate ($7\text{--}10.2\text{--}13.1\text{--}17.3$) \times ($4.1\text{--}6.4\text{--}8.7\text{--}11.8$) μm , mean \pm SD = $11.7 \pm 2.2 \times 7.5 \pm 1.6 \mu\text{m}$, L/W ratio = 1.6. Chlamydospores were not observed.

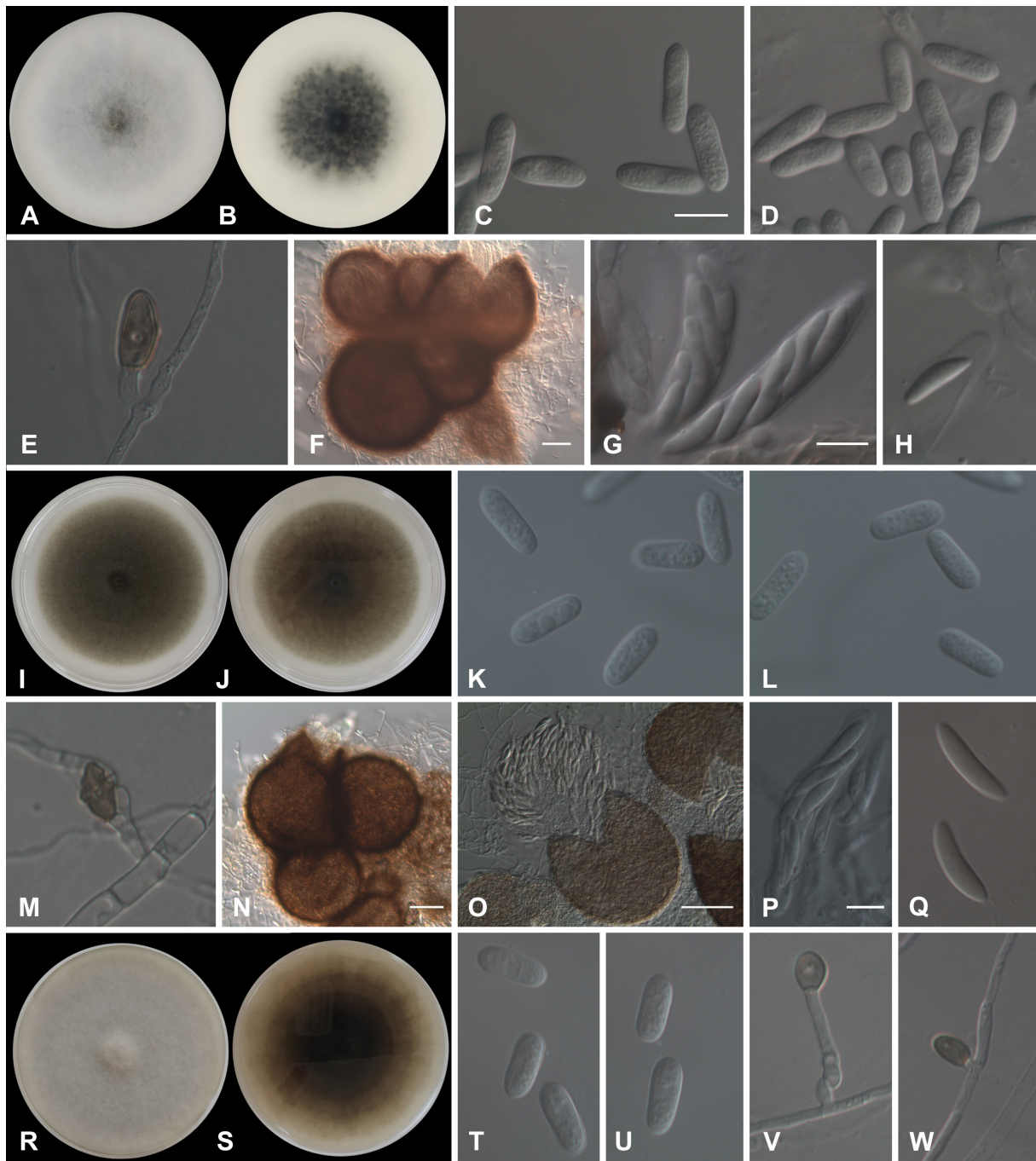


Figure 7. Morphological and cultural characters of *Colletotrichum* isolates from the gloeosporioides complex: *C. alienum* isolate 19331 (A–H); *C. cigarro* isolate 19151 (I–Q); *C. gloeosporioides* isolate 19175 (R–W). Colonies on PDA, upper (A,I,R) and reverse (B,J,S) sides. Conidia (C,D,K,L,T,U) and appressoria (E,M,V,W) on SNA. Perithecia (F,N,O), asci (G,P), and ascospores (H, Q) from MSM with toothpicks. Scale bars: 50 μ m (F,N,O), 10 μ m (C,G,P). Scale bar of (C) applies to (D,E,H,K–M,Q,T–W).

Culture characteristics: Colonies on PDA had a ≥ 75 mm diameter after 7 days at 25 $^{\circ}$ C, and were flat with the entire margin being surface olivaceous gray to pale olivaceous gray, and reverse olivaceous black to olivaceous gray.

Colletotrichum gloeosporioides (Penz.) Penz. & Sacc., Atti Reale Ist. Veneto Sci. Lett. Arti., Serie 6, 2: 670. 1884 (Figure 7R–W).

A sexual morph was not observed. An asexual morph was observed on SNA. Setae were not observed. Conidia were hyaline, smooth-walled, aseptate, straight, and cylindrical

with rounded ends $(11.3\text{--}13.6\text{--}15.6\text{--}17.6) \times (4.7\text{--}5.5\text{--}6\text{--}6.6) \mu\text{m}$ mean \pm SD = $14.6 \pm 1.3 \times 5.7 \pm 0.4 \mu\text{m}$. L/W ratio = 2.5. Appressoria were solitary, brown or dark brown, smooth-walled, with an ovoid-to-ellipsoidal outline, with the entire edge being $(6.5\text{--}7.8\text{--}9.8\text{--}11) \times (4.5\text{--}5.7\text{--}7.3\text{--}8.9) \mu\text{m}$, mean \pm SD = $8.7 \pm 1.2 \times 6.6 \pm 1.1 \mu\text{m}$, L/W ratio = 1.3. Chlamydospores were not observed.

Culture characteristics: Colonies on PDA were ≥ 75 mm after 7 days at 25 °C, and flat with the entire margin surface being pale vinaceous gray, olivaceous gray to white, and the reverse being the same color.

3.4. Population Structure

Based on the molecular and morphological characterization conducted, it was possible to assign a *Colletotrichum* species to the 212 isolates (52 in 2018 and 160 in 2019) obtained in the surveys. Most of the isolates were identified as *C. nymphaeae* ($n = 154$, of which 38 were obtained in 2018 and 116 in 2019), 19 isolates were assigned to *C. acutatum* (6 in 2018 and 13 in 2019), 19 isolates clustered with *C. godetiae* (6 in 2018 and 13 in 2019), 8 isolates were ascribed to *C. gloeosporioides* (1 in 2018 and 7 in 2019), 7 isolates to *C. cigarro* (1 in 2018 and 6 in 2019), 4 as *C. fiorinia*, all obtained in 2019, and 1 to *C. alienum* (2019) (Table S1).

Isolates of *C. nymphaeae* ($n = 154$) were obtained from all the regions surveyed, being the most prevalent species in the country (72.6%), ranging from 43% in the Algarve to 93% in Beira Baixa. From the isolates identified as *C. acutatum* ($n = 19$), ten were from olive trees located in Algarve, representing 27% of the isolates obtained in this region; eight were from Ribatejo e Oeste (11% in this region); and one was from Alentejo. Isolates assigned to *C. godetiae* ($n = 19$) were obtained from olive groves located in Algarve, Alentejo, Ribatejo e Oeste, and Trás-os-Montes. Eight *C. gloeosporioides* isolates were obtained from olive trees grown in Algarve, Alentejo, and Ribatejo e Oeste. Isolates of *C. cigarro* ($n = 7$) were obtained from olives collected in Algarve and Ribatejo e Oeste. The four isolates of *C. fiorinia* were obtained from Algarve, Ribatejo e Oeste, and Beira Baixa. One isolate identified as *C. alienum* was obtained from olive fruit collected in Ribatejo e Oeste (municipality of Caldas da Rainha) (Figures 1, 2 and 8).

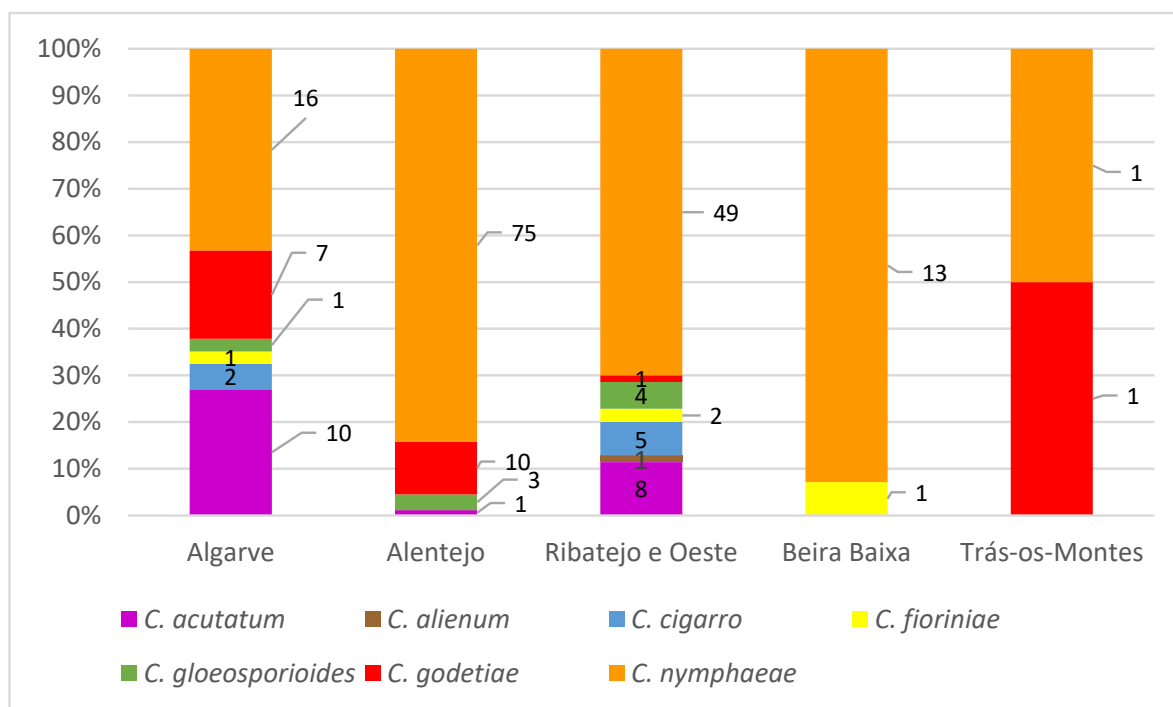


Figure 8. Frequency of *Colletotrichum* spp. associated with olive anthracnose in different districts of Portugal obtained from the surveys in 2018 and 2019.

The population structure of *Colletotrichum* species obtained in the Algarve and Ribatejo e Oeste regions was more diversified than that found in any other regions surveyed. From the 120 sites surveyed at Trás-os-Montes, only two isolates were obtained, so it was not possible to determine the population structure in this region (Figures 1, 2 and 8).

Concerning the host of origin, isolates of *C. nymphaeae* were obtained from all olive cultivars and from oleaster (*Olea europaea* ssp. *europaea* var. *sylvestris*), although they were not isolated from ‘Maçanilha’ (Figure 9). This species was the most frequent anthracnose pathogen on ‘Galega Vulgar’ (84% of isolates) and on ‘Cordovil de Serpa’ (86% of isolates). In contrast, *C. godetiae* represents 75% of the isolates obtained from ‘Arbequina’ and 40% of those from ‘Maçanilha’, while this species represents only 2.7% of the strains isolated from ‘Galega Vulgar’. Similarly, *C. acutatum* represents 40% of the strains isolated from ‘Maçanilha’, but only 6.6% of those from ‘Galega Vulgar’. Considering the pathogen, *C. nymphaeae* was more frequently isolated from ‘Galega Vulgar’ (92% of all *C. nymphaeae* strains were obtained from this cultivar) than any other species: 83% of *C. acutatum* strains were obtained from ‘Galega Vulgar’, along with *C. gloeosporioides* (also 83%), and followed by *C. fiorinia* (67%), *C. cigarro* (50%), and *C. godetiae* (40%).

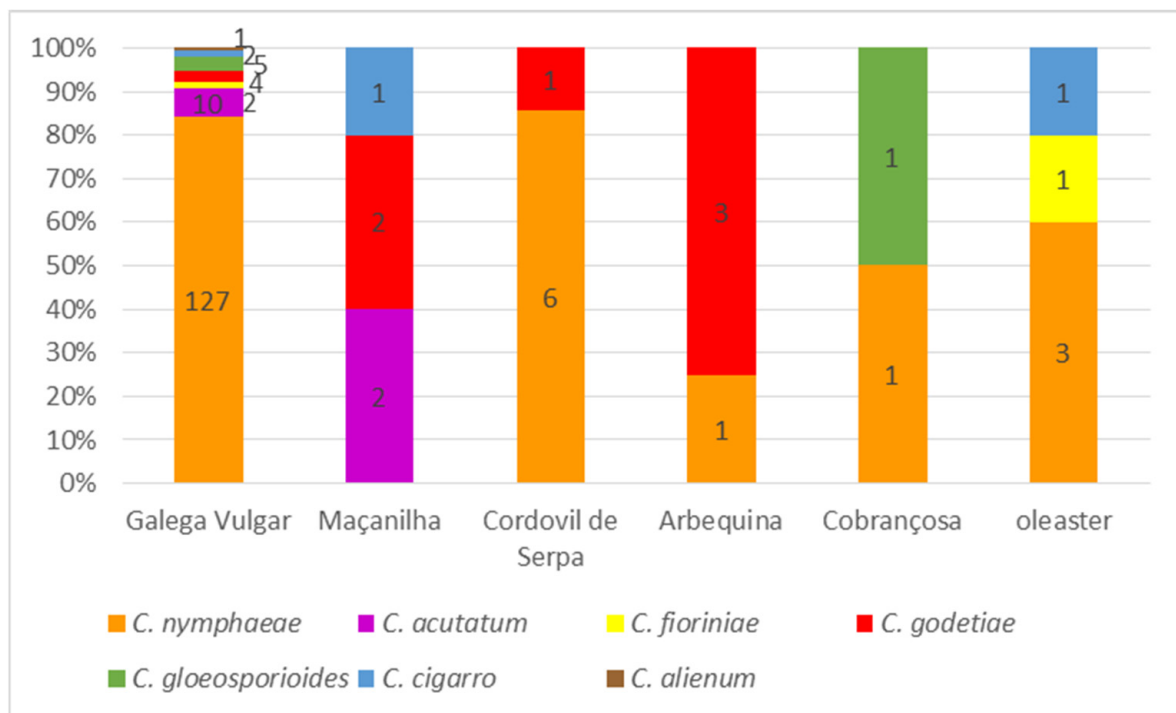


Figure 9. Frequency of *Colletotrichum* spp. associated with olive anthracnose according to olive cultivars (and oleaster) obtained from the surveys of 2018 and 2019.

Besides comparing the results for disease presence and pathogen identity on a regional scale or according to the host cultivar, the fact that several sites were surveyed in both years enables a direct comparison of those parameters at a local scale (Table S4). The presence of symptoms in the field or its development upon incubation in these 23 sites follows the regional patterns described above. In no location have there been shifts in pathogen species; although, in 2019, in a couple of locations at Alentejo, *C. godetiae* co-occurred along with *C. nymphaeae*, whereas a similar situation occurred in Algarve with *C. nymphaeae* and *C. acutatum*.

3.5. Pathogenicity on Detached Olive Fruit

The first symptoms on the inoculated fruit started 4–5 days after inoculation (dai) for the 12 isolates of *Colletotrichum* tested, although differences in the disease progress

were observed among isolates. For instance, 55% of the inoculated fruit with the isolate 19112 of *C. nymphaeae* (at 9 dai) exhibited abundant spore masses expanding away from the inoculation point (rated 5 on the 0–6 scale) and the calculated rAUDPC was 67%, while most of the fruits inoculated with isolates of *C. alienum* (19331), *C. cigarro* (18312B, 19148, 19151, 19300, 19329B and 19330A), *C. gloeosporioides* (19175), and *C. godetiae* (19165) were rated 2 and 3 with the rAUDPC ranging between 38 and 52%. The isolates of *C. acutatum* (19301A) and *C. fiorinia* (19124A) were mostly rated three and four, with the rAUDPC being approximately 60%.

At 15 dai, most of the fruits inoculated with *C. nymphaeae* (19112) were completely rotted, showing abundant conidia in gelatinous matrices (soapy fruit), and the rAUDPC was 73% (DSI = 89%), while for fruit inoculated with the isolates of *C. alienum*, *C. cigarro*, *C. gloeosporioides*, and *C. godetiae*, the rAUDPC ranged between 42 and 57% (DSI = 54–75%), and for the isolates of *C. acutatum* and *C. fiorinia* between 76 and 80% (DSI = 76–81%), respectively. These results suggest that *C. nymphaeae* is capable of inducing anthracnose symptoms in olive fruit from the cultivar ‘Galega Vulgar’ earlier than any of the other species tested in this study. At the end of the experiments, the inoculated fruit showed typical anthracnose symptoms with the rAUDPC ranging from 57 to 85% (DSI = 76–96%), and perithecia were observed on the fruit inoculated with the isolates of *C. alienum* and *C. cigarro*. Koch’s postulates were fulfilled as fungi with the same morpho-cultural and phylogenetic characteristics of the inoculated isolates were re-isolated from fruit, and never from the controls, indicating that these species are able to cause anthracnose disease on the olive fruit (Figures 10 and 11).

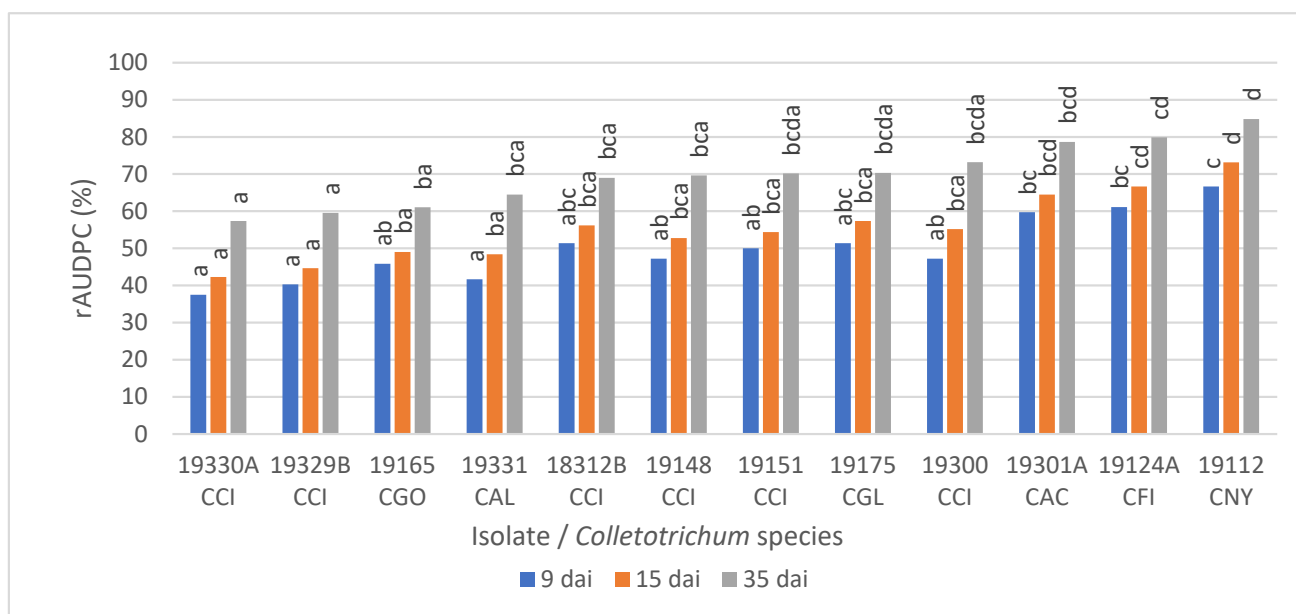


Figure 10. Relative area under the disease progress curve (rAUDPC) for olive fruit of cultivar ‘Galega Vulgar’ inoculated with isolates of *Colletotrichum acutatum* (CAC), *C. alienum* (CAL), *C. cigarro* (CCI), *C. fiorinia* (CFI), *C. gloeosporioides* (CGL), *C. godetiae* (CGO), or *C. nymphaeae* (CNY). Disease severity was assessed 9, 15, and 35 days after inoculation (dai) by using a 0 to 6 rating scale. Columns are the means of two independent assays with 12 inoculated fruits, per isolate each. For each dai, isolates with the same letter do not differ significantly according to Tukey’s honestly significant difference test at $p = 0.05$.

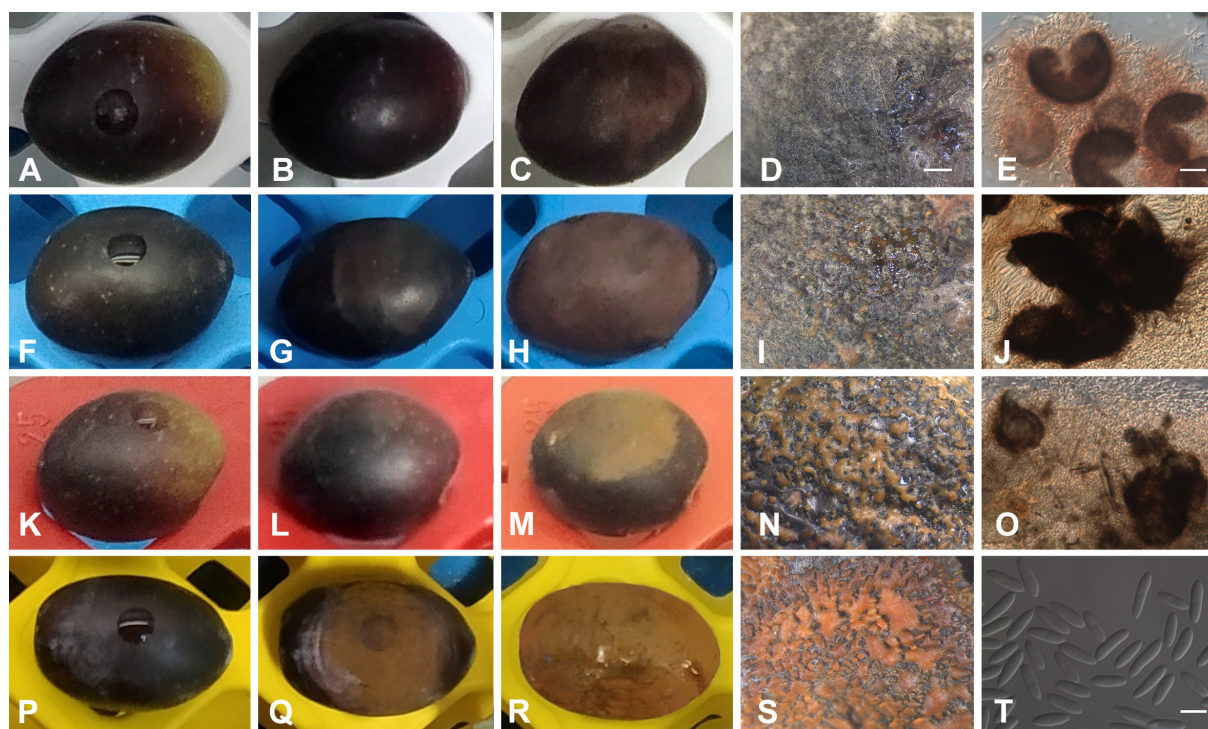


Figure 11. Detached ‘Galega Vulgar’ olive fruits inoculated with *Colletotrichum* isolates: 19331 of *C. alienum* (A–E); 18312B (F–J) and 19300 (K–O) of *C. cigarro*; 19112 (P–T) of *C. nymphaeae*; on inoculation day (A,F,K,P); 9 days after inoculation (dai) (B,G,L,Q); 15 dai (C,H,M,R); 35 dai (D,E,I,J,N,O,S,T). Perithecia, asci, ascospores, and conidia obtained from the inoculated fruit at 35 dai (E,J,O) and conidia (T). Scale bars: 1 mm (D), 50 μ m (E) and 10 μ m (T). Scale bar (D) also applies to (I,N,S) and (E) also applies to (J,O).

4. Discussion

Olive anthracnose has been known in the Iberian Peninsula for centuries and the disease is consistently found in neglected olive groves, even in unfavorable autumns, increasing in incidence and severity under favorable environmental conditions [3]. In Portugal, studies conducted in the first decade of the 21st century showed an average disease incidence of 41% (i.e., anthracnose symptoms found in nearly half of the olive groves surveyed), with another 14% of sites showing the asymptomatic presence of inoculum [11]. In the present study, the disease incidence recorded in Portugal was 4% in 2018 and 29% in 2019. The asymptomatic presence of inoculum was detected in 13% of sites in 2018 and 29% in 2019. These represent situations where no disease was reported but where the fungus was present and potentially capable of causing disease if favorable conditions occurred (wet periods in the field or infection events during fruit storage or transport). Olive anthracnose incidence in Portugal in 2018 and 2019 was lower than the average from the previous decade, and this can be related to autumn rainfall being consistently lower than the average in general and specifically over those two years. The differences in disease incidence between 2018 and 2019 could also be correlated to the temperature values by the end of winter, as mean temperatures in Portugal were below average in February and March 2018 and above average in the same months in 2019. After harvest in autumn, olive anthracnose inoculum is reported to remain on leaves and branches, where conidia are able to survive and undergo secondary conidiation [11], although inoculum levels decrease over summer presumably because of hot and dry conditions. In contrast, above-average temperatures in late winter, when air humidity is still high (typically reaching saturation during the night), may favor inoculum survival and multiplication on leaves and branches, as reported for other pathosystems [18] and as empirically suggested regarding olive anthracnose [19]. Besides climatic factors, the reduction in anthracnose incidence from the first to the second

decade of the century can also be related to the profound changes in olive cropping systems, both because cultivars less susceptible to anthracnose (such as 'Arbequina' and 'Arbosana') and are being implemented in high-density olive groves (displacing the highly susceptible 'Galega Vulgar', which is not well adapted to hedge systems) and because such high-profit systems allow a higher number of fungicide treatments than traditional olive groves.

In the present study, a collection of 212 *Colletotrichum* isolates obtained from olive fruit in the main olive-growing regions of Portugal ($n = 525$ sites; two-year survey) was characterized, based on morphological, molecular, and pathogenicity traits. Despite the value of morphological data, phylogenetic analyses were necessary to properly identify *Colletotrichum* species, especially those included in the acutatum, boninense, and gloeosporioides species complexes. Due to the high number of isolates obtained, we carried out a first screening of species complexes or presumptive species present in our collection using morphological data and ISSR analysis ($n = 212$ isolates). After this step, which made it possible to group the isolates into the acutatum and gloeosporioides species complexes, and sometimes into species, representative isolates from each group were selected for phylogenetic analyses ($n = 47$ isolates). None of the isolates obtained in the present study were grouped into the boninense complex.

The delimitation of species in the genus *Colletotrichum* based on morphology and ITS phylogeny is uncertain; hence, it is recommended to combine multi-gene phylogenetic analysis with morphological descriptions [8,9,51]. In addition to morphology and ITS, loci such as ACT, CHS-1, GAPDH, HIS3, and TUB2 have been recommended to resolve species in the acutatum complex, with GAPDH and TUB2 showing a better performance in species recognition [8]. For the gloeosporioides complex, an additional three loci are used (ApMAT, CAL, and GS; [9,52]), among which ApMAT and GS have been recommended as sufficient to identify species in this complex [52]. Based on phylogenetic analyses and morphological characteristics, our results revealed that *Colletotrichum* isolates collected from olive fruit in our survey belonged to seven species, *C. acutatum*, *C. fiorinae*, *C. godetiae*, and *C. nymphaeae* in the acutatum complex, whereby *C. nymphaeae* was the most prevalent, and *C. alienum*, *C. cigarro*, and *C. gloeosporioides* were present in the gloeosporioides complex.

In fungal plant pathogens, insufficient taxon sampling in combination with low taxonomic resolution are among the main reasons for the ambiguity of species boundaries. When a new species is described, it is necessary to follow some guidelines to avoid an inflation of taxonomic issues with the introduction of invalid and unnecessary names [53]. Two examples are the species *C. orientale* (as 'orientalis') [54] and *C. radermacherae* [55] that were reduced to synonyms of *C. fiorinae* in a recent study [56] because the morphological differences observed between the ex-type strains of these three species were not considered sufficient to distinguish them as different species, also corroborated by less than 2% differences in the nucleotide sequences of five loci (ACT, CHS-1, GAPDH, ITS, and TUB2).

In our phylogenetic analysis, aiming to reflect the intraspecific variability within *C. nymphaeae* [8] sequences, 27 strains of this species were retrieved from GenBank, including three strains initially assigned to *C. citri* [57] and synonymized with *C. nymphaeae* [50]. From this analysis, *C. simulanticitri* [49] was also grouped in the *C. nymphaeae* clade and is, most probably, another synonym of *C. nymphaeae*. To reinforce this statement, it should be stressed that only four nucleotide differences were found between the ex-type strains of *C. nymphaeae* (CBS 515.78) and *C. simulanticitri* (YMF1.07302) in the four loci available for the latter species (ACT, CHS-1, GAPDH, and ITS), which is less than the nucleotide differences observed between CBS 515.78 and CBS 127608 or IMI 360386 that were assigned to *C. nymphaeae* by our multi-locus phylogenetic analyses and by coalescent-based species delimitation methods (PTP, mPTP, and BPP) [8,58]

In this study seven isolates were identified as *C. cigarro*, a putative cryptic species complex. The species limits between *C. cigarro* and the neighboring *C. fructivorum*, *C. hedericola*, *C. helleniense*, *C. jiangxiense*, *C. kahawae* and *C. rhexiae* are still not well established and more in-depth studies are needed [59,60].

The virulence diversity of isolates representing *C. acutatum*, *C. fioriniae*, *C. godetiae*, *C. nymphaeae*, and *C. gloeosporioides* obtained in Portugal was previously evaluated in several olive cultivars, including 'Galega Vulgar'. Although cultivar × pathogen interactions occurred, 'Galega Vulgar' proved to be one of the most susceptible cultivars to anthracnose [15]. In the present pathogenicity studies, these species were represented by only one isolate each (positive controls) because our main objective was to demonstrate the pathogenicity of the species *C. cigarro* and *C. alienum*, until now unknown as causal agents of olive anthracnose in Portugal. For this reason, in addition to the species mentioned above, the pathogenicity studies included a higher number of representative isolates of *C. cigarro* ($n = 6$) and only one in the case of *C. alienum*, as it corresponded to the only isolate obtained by us. Taken together, all isolates of *C. cigarro* proved to be pathogenic on olive fruit, with no significant differences between the isolates, although two of them (19030A and 19329B) proved to be significantly less virulent than *C. acutatum*, *C. fioriniae*, and *C. nymphaeae*. Nevertheless, these two isolates of *C. cigarro* were not significantly different from *C. godetiae*, *C. alienum*, or *C. gloeosporioides*. Similar virulence patterns between *C. cigarro* and *C. gloeosporioides* were observed in pathogenicity tests carried out on Italian olive cultivars, with those species being less virulent than *C. acutatum* [61]. In the present study, an intermediate behavior was recorded for *C. alienum*, being less virulent than *C. acutatum*, *C. fioriniae*, and *C. nymphaeae* at 9 dai, or than *C. fioriniae* and *C. nymphaeae* at 15 dai, or even than *C. nymphaeae* at 35 dai. Even so, the virulence of *C. alienum* was comparable to that of *C. godetiae* or *C. gloeosporioides*. *Colletotrichum alienum* was reported for the first time as one of the causal agents of olive anthracnose in Uruguay, being responsible, when inoculated on flowers and fruit, for disease incidence values comparable to those obtained upon inoculation with *C. acutatum*, *C. fioriniae*, *C. nymphaeae*, or *C. theobromicola* [23]. It should be noted that *C. nymphaeae* was significantly more virulent towards 'Galega Vulgar' fruit than *C. godetiae*, at any time after inoculation, which confirms our previous findings [15], but it contrasts with the results obtained by other authors in which *C. godetiae* was more virulent than *C. nymphaeae* on this same olive cultivar [17]. This apparent inconsistency could be explained either by reasons inherent to intraspecific variability or by small differences between experimental procedures (e.g., fruit ripeness, inoculation method, and incubation temperature). Although tested on different olive cultivars, also in Italy, *C. nymphaeae* revealed greater virulence than *C. godetiae* and a virulence comparable to that of *C. acutatum*, [16], which is in line with our results.

The present study revealed *C. nymphaeae* as the most common olive anthracnose pathogen in Portugal, representing 73% of the 212 isolates analyzed, occurring in all regions surveyed and presenting a clear preference for 'Galega Vulgar'. This prevalence follows the scenario depicted in the first decade of the 21st century, when *C. nymphaeae* accounted for 80% of the isolates associated with olive anthracnose [11]. By then, it was shown that *C. nymphaeae* was even more frequent in years with a higher disease incidence (probably due to its high virulence), and the lower frequency of isolation of *C. nymphaeae* in the present study may be related to the low disease incidence in 2018 and 2019. *Colletotrichum nymphaeae* associated with olive anthracnose is mostly restricted to southwestern Iberia [11,14,62,63], but has more recently been reported in northeastern Italy [21], Uruguay [23], and Brazil [64]. As one of the most virulent olive anthracnose pathogens [15], *C. nymphaeae* may become more impactful in the future and continue its spread to other olive-growing regions, as well as to other crops. To this end, it is worth stressing that *C. nymphaeae* has ca. 50 host plant species, in some cases is the most important anthracnose pathogen (e.g., strawberry anthracnose), and seems to be expanding geographically (e.g., numerous reports on diverse hosts in the American continent in recent years) [65].

Colletotrichum godetiae represents 9% of the olive anthracnose isolates analyzed in this study. This fungus was detected in all regions surveyed except Beira Baixa. These results follow those previously obtained (12% isolates in the 2000s) [11], although the low level of anthracnose detection at Trás-os-Montes in the present study (relatable to a combination of less favorable environmental conditions and the use of less susceptible cultivars, as

previously discussed [11]) does not enable us to confirm if this species is still the most common in that region. Although less virulent than *C. nymphaeae* or *C. acutatum*, *C. godetiae* is still considered the most common olive anthracnose pathogen in the Mediterranean basin [4,17] and its current epidemic status in intensive almond orchards [66] raises concern about cross-infection from and to olive. In fact, *C. godetiae* is hosted by ca. 40 plant species, including other fruit crops such as apple, peach, and strawberry. As opposed to *C. nymphaeae*, this species is mostly restricted to Europe [65].

As for *C. godetiae*, *C. acutatum* also represents 9% of the olive anthracnose isolates analyzed in this study and was recorded in the Algarve, Alentejo, and Ribatejo e Oeste regions. In the past, this fungus accounted for 3.6% of isolates associated with olive anthracnose in Portugal and was restricted to the Algarve. Although this fungus is still common and is even expanding at the Algarve, where it represents 27% of the isolates (20% in the previous study), it has now been reported in Alentejo (a single isolate from Vila Alva, Cuba—interestingly, one of the refuge areas for olive anthracnose, where the disease is recorded even in unfavorable years) and in eight isolates from Ribatejo e Oeste (mostly from the Torres Novas–Tomar–Abrantes triangle, an area where both traditional and high-density olive groves are common). This geographic expansion is in line with the spread of this pathogen as an olive anthracnose pathogen in several countries. Known for a long time as a causal agent of olive anthracnose in South Africa and Australia [3,67], and reported as one of the most virulent olive anthracnose pathogens [15], this fungus is now reported in Mediterranean countries such as Italy, Albania, Greece, and Tunisia [13,61,68–70], and also in Pakistan [71], often as the most frequent pathogen and displacing other species, such as in parts of Italy and in Tunisia [3]. Although *C. acutatum* occurs on ca. 40 host species, this species seemed to be restricted to Oceania and Africa, and only recently expanded to the Mediterranean region on several other tree crops (almond, chestnut, citrus, and pomegranate) [65]. More recently, it expanded into the American continent, where it became the prevalent olive anthracnose pathogen in Uruguay [23] and also appeared associated with olive blossom blight and olive anthracnose in Brazil [64]. Given the rapid geographic expansion of *C. acutatum*, it is likely that it will become more important in the near future, not only as an olive anthracnose pathogen, but also as a pathogen of other crops.

In this study, eight *C. gloeosporioides* isolates were identified from the Algarve, Alentejo, and Ribatejo e Oeste regions. Coincidentally, the frequency of detection of this species in the current study was precisely the same as that in the study conducted in the first decade of the 21st century: 3.8% [11]. *Colletotrichum gloeosporioides* is a widely polyphagous fungus (over 100 host species [65]), but it is not a highly virulent pathogen towards olives [15].

In this study, *C. cigarro* is recorded for the first time in Portugal as one of the causal agents of olive anthracnose. This fungus was detected at unrelated sites at the Algarve and at Ribatejo e Oeste. This species had previously been recorded as being associated with olive anthracnose in Italy and Australia [9,20,61]. Given the polyphagous nature of this fungus (ca. 30 host species [65]), current results raise concern about the future relevance of this fungus regarding anthracnose on olive and on other crops.

Four *C. fiorinae* isolates were identified in this study, scattered over the Algarve, Ribatejo e Oeste, and Beira Baixa, and maintaining the distribution pattern depicted in the past [11]. Although very common (namely in temperate regions), *C. fiorinae* most frequently occurs among other *Colletotrichum* species, being a less important pathogen on many of its ca. 80 host species [65]. This seems to be the case with *C. fiorinae* associated with olive anthracnose in Portugal as well as in different parts of the world: Australia, Italy, Turkey, and the USA [4,11,13,14,72]. Nevertheless, *C. fiorinae* is consistently placed as an important pathogen associated with apple bitter rotting [65], and the detection of one of the isolates in the present study in an apple growing area (Caldas da Rainha) raises concern regarding this fruit crop.

A single *C. alienum* isolate was detected in this study, also at Caldas da Rainha. This is the first report of olive anthracnose caused by *C. alienum* in Portugal and in the Northern

Hemisphere, as previous records were from Australia and Uruguay [4,23]. In fact, previous records of this fungus in Portugal and Europe are limited to the Proteaceae [73], and the European Food Safety Authority has performed a pest categorization for this fungus considering its potential danger towards fruit crops, such as apple, avocado, mango, persimmon, and strawberry [74].

This study suggests that the incidence of olive anthracnose in Portugal is declining, which may be related to climate change, and specifically to a reduction in rainfall in autumn, and to the use of less susceptible cultivars under high-density systems with an increased use of fungicides to control the main leaf and fruit diseases of olive. The population structure of *Colletotrichum* spp. remains dominated by *C. nymphaeae*, an olive pathogen traditionally restricted to southwestern Iberia but that is now becoming of concern in other parts of the world. *Colletotrichum acutatum*, previously associated with olive anthracnose only in the Southern Hemisphere and later in the Algarve region of Portugal, has recently spread as an important pathogen in much of the Mediterranean basin and is also territorially spreading in Portugal. Conclusions from this study highlight the importance of detailed etiological and mycological studies, resulting in the pinpointing of less frequent pathogens, as in the case of *C. alienum*, that may help to anticipate future problems for olive and other crops.

Supplementary Materials: The following supporting information can be downloaded at <https://www.mdpi.com/article/10.3390/horticulturae10050434/s1>, Figure S1: Dendrogram with the phylogenetic relationships among the *Colletotrichum* isolates calculated according to the Dice coefficient and the agglomerative method UPGMA from the profile data generated with Inter Simple Sequence Repeat (ISSR) primers (AG)₈YT (Y = C + T) and (CAG)₅. A total of 2000 bootstrap replicates were used; Table S1: Information about the *Colletotrichum* isolates analyzed with the primers (AG)₈YT (Y = C + T) and (CAG)₅. Isolates used as references in the Inter Simple Sequence Repeat (ISSR) analysis are emphasized in bold type. * = Ex-type strain; Table S2: Isolates and reference strains used in this study, with collection details and GenBank accession numbers (newly generated sequences are indicated in bold); Table S3: Binary matrix representing the absence (0) or presence (1) of a DNA fragment generated by the Inter Simple Sequence Repeat (ISSR) primers (AG)₈YT and (CAG)₅ for the 212 *Colletotrichum* isolates obtained in Portugal and for the 19 *Colletotrichum* isolates used as reference isolates in this study; Table S4: Presence of olive anthracnose symptoms and pathogen identification in the 2018 and 2019 surveys conducted in 23 locations representing different types of olive groves with diverse cultivars located at Beira Baixa [1], Alentejo [2–17], and Algarve [18–23].

Author Contributions: Conceptualization, A.C., P.T. and H.O.; Formal Analysis, A.C.; Funding acquisition, H.O.; Investigation, A.C., T.N., H.G.A., A.L., P.T. and H.O.; Methodology, A.C. and T.N.; Project Administration, H.O.; Software, A.C.; Validation, A.C., P.T. and H.O.; Writing—Original Draft, A.C., P.T. and H.O.; Writing—Review and Editing, A.C., T.N., H.G.A., A.L., P.T. and H.O. All authors have read and agreed to the published version of the manuscript.

Funding: This work was funded by national funds through FCT—Fundação para a Ciência e a Tecnologia, I.P., Portugal, under the projects PTDC/ASP-PLA/28547/2017 and UIDB/04129/2020 of the LEAF-Linking Landscape, Environment, Agriculture and Food, Research Unit. Ana Cabral (DL 57/2016/CP1382/CT0010), Andreia Loureiro (DL 57/2016/CP1382/CT0014), and Pedro Talhinhos (DL 57/2016/CP1382/CT0023) were funded by national (Portuguese) funds (OE), through FCT, I.P., in the scope of the framework contract foreseen in numbers 4–6 of article-23, of the Decree-Law 57/2016, 29 August, changed by Law 57/2017, 19 July.

Data Availability Statement: All sequences generated in this study have been submitted to NCBI GenBank (accessions numbers PP506774-PP506995 and PP508293-PP508342). The sequence alignments, and phylogenetic inference output files from this study are available in TreeBase study number S31264.

Acknowledgments: The authors would like to thank Fátima Peres and Nuno Conceição, members of the Project PTDC/ASP-PLA/28547/2017, for their help in collecting samples.

Conflicts of Interest: The authors declare no conflicts of interest. The funders had no role in the design of the study; in the collection, analyses, or interpretation of data; in the writing of the manuscript; or in the decision to publish the results.

References

1. Food and Agricultural Organisation of the United Nations, FAOSTAT-Crops and Livestock Products. Available online: <https://www.fao.org/faostat/en/#data/QCL/visualize> (accessed on 6 February 2024).
2. Superfície das Principais Culturas Agrícolas (ha) por Localização Geográfica (Região Agrária) e Espécie; Anual-INE, Estatísticas da Produção Vegetal. Available online: https://www.ine.pt/xportal/xmain?xpid=INE&xpgid=ine_indicadores&indOcorrCod=0000019 (accessed on 6 February 2024).
3. Talhinhos, P.; Loureiro, A.; Oliveira, H. Olive Anthracnose: A Yield- and Oil Quality-degrading Disease Caused by Several Species of *Colletotrichum* that Differ in Virulence, Host Preference and Geographical Distribution. *Mol. Plant Pathol.* **2018**, *19*, 1797–1807. [[CrossRef](#)]
4. Moral, J.; Agustí-Brisach, C.; Raya, M.C.; Jurado-Bello, J.; López-Moral, A.; Roca, L.F.; Chattaoui, M.; Rhouma, A.; Nigro, F.; Sergeeva, V.; et al. Diversity of *Colletotrichum* Species Associated with Olive Anthracnose Worldwide. *J. Fungi* **2021**, *7*, 741. [[CrossRef](#)] [[PubMed](#)]
5. Peres, F.; Talhinhos, P.; Afonso, H.; Alegre, H.; Oliveira, H.; Ferreira-Dias, S. Olive Oils from Fruits Infected with Different Anthracnose Pathogens Show Sensory Defects Earlier Than Chemical Degradation. *Agronomy* **2021**, *11*, 1041. [[CrossRef](#)]
6. Moral, J.; Xaviér, C.; Roca, L.F.; Romero, J.; Moreda, W.; Trapero, A. La Antracnosis Del Olivo y Su Efecto En La Calidad Del Aceite. *Grasas Aceites* **2014**, *65*, e028. [[CrossRef](#)]
7. Damm, U.; Cannon, P.F.; Woudenberg, J.H.C.; Johnston, P.R.; Weir, B.S.; Tan, Y.P.; Shivas, R.G.; Crous, P.W. The *Colletotrichum boninense* Species Complex. *Stud. Mycol.* **2012**, *73*, 1–36. [[CrossRef](#)] [[PubMed](#)]
8. Damm, U.; Cannon, P.F.; Woudenberg, J.H.C.; Crous, P.W. The *Colletotrichum acutatum* Species Complex. *Stud. Mycol.* **2012**, *73*, 37–113. [[CrossRef](#)] [[PubMed](#)]
9. Weir, B.S.; Johnston, P.R.; Damm, U. The *Colletotrichum gloeosporioides* Species Complex. *Stud. Mycol.* **2012**, *73*, 115–180. [[CrossRef](#)] [[PubMed](#)]
10. Talhinhos, P.; Neves-Martins, J.; Oliveira, H.; Sreenivasaprasad, S. The Distinctive Population Structure of *Colletotrichum* Species Associated with Olive Anthracnose in the Algarve Region of Portugal Reflects a Host-Pathogen Diversity Hot Spot. *FEMS Microbiol. Lett.* **2009**, *296*, 31–38. [[CrossRef](#)]
11. Talhinhos, P.; Mota-Capitão, C.; Martins, S.; Ramos, A.P.; Neves-Martins, J.; Guerra-Guimarães, L.; Várzea, V.; Silva, M.C.; Sreenivasaprasad, S.; Oliveira, H. Epidemiology, Histopathology and Aetiology of Olive Anthracnose Caused by *Colletotrichum acutatum* and *C. gloeosporioides* in Portugal. *Plant Pathol.* **2011**, *60*, 483–495. [[CrossRef](#)]
12. Cacciola, S.O.; Faedda, R.; Fulvia, S.; Agosteo, G.E.; Schena, L.; Frisullo, S.; Magnano di San Lio, G. Olive Anthracnose. *J. Plant Pathol.* **2012**, *94*, 29–44.
13. Mosca, S.; Li Destri Nicosia, M.G.; Cacciola, S.O.; Schena, L. Molecular Analysis of *Colletotrichum* Species in the Carposphere and Phyllosphere of Olive. *PLoS ONE* **2014**, *9*, e114031. [[CrossRef](#)] [[PubMed](#)]
14. Talhinhos, P.; Sreenivasaprasad, S.; Neves-Martins, J.; Oliveira, H. Molecular and Phenotypic Analyses Reveal Association of Diverse *Colletotrichum acutatum* Groups and a Low Level of *C. gloeosporioides* with Olive Anthracnose. *Appl. Environ. Microbiol.* **2005**, *71*, 2987–2998. [[CrossRef](#)] [[PubMed](#)]
15. Talhinhos, P.; Gonçalves, E.; Sreenivasaprasad, S.; Oliveira, H. Virulence Diversity of Anthracnose Pathogens (*Colletotrichum acutatum* and *C. gloeosporioides* Species Complexes) on Eight Olive Cultivars Commonly Grown in Portugal. *Eur. J. Plant Pathol.* **2015**, *142*, 73–83. [[CrossRef](#)]
16. Riolo, M.; Pane, A.; Santilli, E.; Moricca, S.; Cacciola, S.O. Susceptibility of Italian Olive Cultivars to Various *Colletotrichum* Species Associated with Fruit Anthracnose. *Plant Pathol.* **2023**, *72*, 255–267. [[CrossRef](#)]
17. Garcia-Lopez, M.T.; Serrano, M.S.; Camiletti, B.X.; Gordon, A.; Estudillo, C.; Trapero, A.; Diez, C.M.; Moral, J. Study of the Competition between *Colletotrichum godetiae* and *C. nymphaeae*, Two Pathogenic Species in Olive. *Sci. Rep.* **2023**, *13*, 5344. [[CrossRef](#)] [[PubMed](#)]
18. Velásquez, A.C.; Castroverde, C.D.M.; He, S.Y. Plant–Pathogen Warfare under Changing Climate Conditions. *Curr. Biol.* **2018**, *28*, R619–R634. [[CrossRef](#)] [[PubMed](#)]
19. Pangallo, S.; Li Destri Nicosia, M.G.; Agosteo, G.E.; Schena, L. Control of Olive Anthracnose and Leaf Spot Disease by Bloom Treatments with a Pomegranate Peel Extract. *J. Saudi Soc. Agric. Sci.* **2022**, *21*, 248–254. [[CrossRef](#)]
20. Schena, L.; Abdelfattah, A.; Mosca, S.; Li Destri Nicosia, M.G.; Agosteo, G.E.; Cacciola, S.O. Quantitative Detection of *Colletotrichum godetiae* and *C. acutatum sensu stricto* in the Phyllosphere and Carposphere of Olive during Four Phenological Phases. *Eur. J. Plant Pathol.* **2017**, *149*, 337–347. [[CrossRef](#)]
21. Antelmi, I.; Sion, V.; Nigro, F. First Report of *Colletotrichum nymphaeae* on Olive in Italy. *Plant Dis.* **2019**, *103*, 765. [[CrossRef](#)]
22. Lima, N.B.; Pastor, S.E.; Maza, C.E.; Conforto, C.; Vargas-Gil, S.; Roca, M. First Report of Anthracnose of Olive Fruit Caused by *Colletotrichum theobromicola* in Argentina. *Plant Dis.* **2020**, *104*, 589. [[CrossRef](#)]
23. Moreira, V.; Mondino, P.; Alaniz, S. Olive Anthracnose Caused by *Colletotrichum* in Uruguay: Symptoms, Species Diversity and Pathogenicity on Flowers and Fruits. *Eur. J. Plant Pathol.* **2021**, *160*, 663–681. [[CrossRef](#)]
24. Ceniz, J.L. Rapid Extraction of Fungal DNA for PCR Amplification. *Nucleic Acids Res.* **1992**, *20*, 2380. [[CrossRef](#)] [[PubMed](#)]
25. Zietkiewicz, E.; Rafalski, A.; Labuda, D. Genome Fingerprinting by Simple Sequence Repeat (SSR)-Anchored Polymerase Chain Reaction Amplification. *Genomics* **1994**, *20*, 176–183. [[CrossRef](#)] [[PubMed](#)]

26. Rodriguez, R.J.; Yoder, O.C. A Family of Conserved Repetitive DNA Elements from the Fungal Plant Pathogen *Glomerella cingulata* (*Colletotrichum lindemuthianum*). *Exp. Mycol.* **1991**, *15*, 232–242. [[CrossRef](#)]
27. Reis, P.; Cabral, A.; Nascimento, T.; Oliveira, H. Diversity of *Ilyonectria* Species in a Young Vineyard Affected by Black Foot Disease. *Phytopathol. Mediterr.* **2013**, *52*, 335–346.
28. Talhinhos, P.; Sreenivasaprasad, S.; Neves-Martins, J.; Oliveira, H. Genetic and Morphological Characterization of *Colletotrichum acutatum* Causing Anthracnose of Lupins. *Phytopathology* **2002**, *92*, 986–996. [[CrossRef](#)] [[PubMed](#)]
29. Carbone, I.; Kohn, L.M. A Method for Designing Primer Sets for Speciation Studies in Filamentous Ascomycetes. *Mycologia* **1999**, *91*, 553–556. [[CrossRef](#)]
30. O'Donnell, K.; Cigelnik, E. Two Divergent Intragenomic rDNA ITS2 Types within a Monophyletic Lineage of the Fungus *Fusarium* Are Nonorthologous. *Mol. Phylogenet Evol.* **1997**, *7*, 103–116. [[CrossRef](#)] [[PubMed](#)]
31. Glass, N.L.; Donaldson, G.C. Development of Primer Sets Designed for Use with the PCR to Amplify Conserved Genes from Filamentous Ascomycetes. *Appl. Environ. Microbiol.* **1995**, *61*, 1323–1330. [[CrossRef](#)]
32. Crous, P.W.; Groenewald, J.Z.; Risède, J.-M.; Simoneau, P.; Hywel-Jones, N.L. *Calonectria* Species and Their *Cylindrocladium* Anamorphs: Species with Sphaeropedunculate Vesicles. *Stud. Mycol.* **2004**, *50*, 415–430.
33. de Hoog, G.S.; Gerrits van den Ende, A.H. Molecular Diagnostics of Clinical Strains of Filamentous Basidiomycetes. *Mycoses* **1998**, *41*, 183–189. [[CrossRef](#)] [[PubMed](#)]
34. White, T.J.; Bruns, T.; Lee, S.; Taylor, J. Amplification and Direct Sequencing of Fungal Ribosomal RNA Genes for Phylogenetics. PCR Protocols: A Guide to Methods and Applications. In *PCR Protocols*; Academic Press, Inc.: New York, NY, USA, 1990.
35. Guerber, J.C.; Liu, B.; Correll, J.C.; Johnston, P.R. Characterization of Diversity in *Colletotrichum acutatum sensu lato* by Sequence Analysis of Two Gene Introns, mtDNA and Intron RFLPs, and Mating Compatibility. *Mycologia* **2003**, *95*, 872–895. [[CrossRef](#)] [[PubMed](#)]
36. Stephenson, S.A.; Green, J.R.; Manners, J.M.; Maclean, D.J. Cloning and Characterisation of Glutamine Synthetase from *Colletotrichum gloeosporioides* and Demonstration of Elevated Expression during Pathogenesis on *Stylosanthes guianensis*. *Curr. Genet.* **1997**, *31*, 447–454. [[CrossRef](#)] [[PubMed](#)]
37. Silva, D.N.; Talhinhos, P.; Várzea, V.; Cai, L.; Paulo, O.S.; Batista, D. Application of the Apn2/MAT Locus to Improve the Systematics of the *Colletotrichum gloeosporioides* Complex: An Example from Coffee (*Coffea* spp.) Hosts. *Mycologia* **2012**, *104*, 396–409. [[CrossRef](#)] [[PubMed](#)]
38. Katoh, K.; Rozewicki, J.; Yamada, K.D. MAFFT Online Service: Multiple Sequence Alignment, Interactive Sequence Choice and Visualization. *Brief. Bioinform.* **2019**, *20*, 1160–1166. [[CrossRef](#)] [[PubMed](#)]
39. Tamura, K.; Stecher, G.; Kumar, S. MEGA11: Molecular Evolutionary Genetics Analysis Version 11. *Mol. Biol. Evol.* **2021**, *38*, 3022–3027. [[CrossRef](#)] [[PubMed](#)]
40. Vaidya, G.; Lohman, D.J.; Meier, R. SequenceMatrix: Concatenation Software for the Fast Assembly of Multi-Gene Datasets with Character Set and Codon Information. *Cladistics* **2011**, *27*, 171–180. [[CrossRef](#)] [[PubMed](#)]
41. Nylander, J.A.A. *MrModelTest v2 Program Distributed by the Author*; Evolutionary Biology Centre, Uppsala University: Uppsala, Sweden, 2004.
42. Ronquist, F.; Teslenko, M.; van der Mark, P.; Ayres, D.L.; Darling, A.; Höhna, S.; Larget, B.; Liu, L.; Suchard, M.A.; Huelsenbeck, J.P. MrBayes 3.2: Efficient Bayesian Phylogenetic Inference and Model Choice across a Large Model Space. *Syst. Biol.* **2012**, *61*, 539–542. [[CrossRef](#)] [[PubMed](#)]
43. Miller, M.A.; Pfeiffer, W.; Schwartz, T. Creating the CIPRES Science Gateway for Inference of Large Phylogenetic Trees. In Proceedings of the 2010 Gateway Computing Environments Workshop, GCE, New Orleans, LA, USA, 14 November 2010.
44. Nirenberg, H. Untersuchungen Über Die Morphologische Und Biologische Differenzierung in Der Fusarium-Sektion Liseola. *Mitt. Biol. Bundesanst. Land. Forstwirtschaft. Berl. Dahl.* **1976**, *169*, 1–167. [[CrossRef](#)]
45. Rayner, R.W. *A Mycological Colour Chart*; Commonwealth Mycological Institute: Kew, UK, 1970; pp. 1–34.
46. Guerber, J.C.; Correll, J.C. Characterization of *Glomerella acutata*, the Teleomorph of *Colletotrichum acutatum*. *Mycologia* **2001**, *93*, 216–229. [[CrossRef](#)]
47. International Olive Council. Guide for the Determination of the Characteristics of Oil-Olives. COI/OH/Doc. No 1. 2011. Available online: <https://www.internationaloliveoil.org/wp-content/uploads/2019/11/COI-OH-Doc.-1-2011-Eng.pdf> (accessed on 20 March 2024).
48. Madden, L.V.; Hughes, G.; van den Bosch, F. Chapter 4: Temporal Analysis I: Quantifying and Comparing Epidemics. In *The Study of Plant Disease Epidemics*; Madden, L.V., Hughes, G., van den Bosch, F., Eds.; The American Phytopathological Society: St. Paul, MN, USA, 2017; pp. 63–116.
49. Yu, Z.; Jiang, X.; Zheng, H.; Zhang, H.; Qiao, M. Fourteen New Species of Foliar *Colletotrichum* Associated with the Invasive Plant *Ageratina adenophora* and Surrounding Crops. *J. Fungi* **2022**, *8*, 185. [[CrossRef](#)]
50. Damm, U.; Sun, Y.C.; Huang, C.J. *Colletotrichum eriobotryae* sp. nov. and *C. nymphaeae*, the Anthracnose Pathogens of Loquat Fruit in Central Taiwan, and Their Sensitivity to Azoxystrobin. *Mycol. Prog.* **2020**, *19*, 367–380. [[CrossRef](#)]
51. Crouch, J.A.; Clarke, B.B.; Hillman, B.I. What Is the Value of ITS Sequence Data in *Colletotrichum* Systematics and Species Diagnosis? A Case Study Using the Falcate-Spored Graminicolous *Colletotrichum* Group. *Mycologia* **2009**, *101*, 648–656. [[CrossRef](#)]

52. Liu, F.; Weir, B.S.; Damm, U.; Crous, P.W.; Wang, Y.; Liu, B.; Wang, M.; Zhang, M.; Cai, L. Unravelling *Colletotrichum* Species Associated with *Camellia* Employing ApMat and GS Loci to Resolve Species in the *C. gloeosporioides* Complex. *Persoonia* **2015**, *35*, 63–86. [[CrossRef](#)] [[PubMed](#)]
53. Jayawardena, R.S.; Hyde, K.D.; de Farias, A.R.G.; Bhunjun, C.S.; Ferdinandez, H.S.; Manamgoda, D.S.; Udayanga, D.; Herath, I.S.; Thambugala, K.M.; Manawasinghe, I.S.; et al. What Is a Species in Fungal Plant Pathogens? *Fungal Divers.* **2021**, *109*, 239–266. [[CrossRef](#)]
54. Chen, Y.; Fu, D.; Wang, W.; Gleason, M.L.; Zhang, R.; Liang, X.; Sun, G. Diversity of *Colletotrichum* Species Causing Apple Bitter Rot and *Glomerella* Leaf Spot in China. *J. Fungi* **2022**, *8*, 740. [[CrossRef](#)]
55. Zhang, Q.; Nizamani, M.M.; Feng, Y.; Yang, Y.Q.; Jayawardena, R.S.; Hyde, K.D.; Wang, Y.; Li, C. Genome-Scale and Multi-Gene Phylogenetic Analyses of *Colletotrichum* spp. Host Preference and Associated with Medicinal Plants. *Mycosphere* **2023**, *14*, 1–106. [[CrossRef](#)]
56. Zhang, Y.X.; Chen, J.W.; Manawasinghe, I.S.; Lin, Y.H.; Jayawardena, R.S.; Mckenzie, E.H.C.; Hyde, K.D.; Xiang, M.M. Identification and Characterization of *Colletotrichum* Species Associated with Ornamental Plants in Southern China. *Mycosphere* **2023**, *14*, 262–302. [[CrossRef](#)]
57. Huang, F.; Chen, G.Q.; Hou, X.; Fu, Y.S.; Cai, L.; Hyde, K.D.; Li, H.Y. *Colletotrichum* Species Associated with Cultivated Citrus in China. *Fungal Divers.* **2013**, *61*, 61–74. [[CrossRef](#)]
58. Zapata, M.; Rodríguez-Serrano, E.; Castro, J.F.; Santelices, C.; Carrasco-Fernández, J.; Damm, U.; Palfner, G. Novel Species and Records of *Colletotrichum* Associated with Native Woody Plants in South-Central Chile. *Mycol. Prog.* **2024**, *23*, 18. [[CrossRef](#)]
59. Cabral, A.; Azinheira, H.G.; Talhinhos, P.; Batista, D.; Ramos, A.P.; Silva, M.D.C.; Oliveira, H.; Várzea, V. Pathological, Morphological, Cytogenomic, Biochemical and Molecular Data Support the Distinction between *Colletotrichum cigarro* comb. et stat. nov. and *Colletotrichum kahawae*. *Plants* **2020**, *9*, 502. [[CrossRef](#)]
60. Liu, F.; Ma, Z.Y.; Hou, L.W.; Diao, Y.Z.; Wu, W.P.; Damm, U.; Song, S.; Cai, L. Updating Species Diversity of *Colletotrichum*, with a Phylogenomic Overview. *Stud. Mycol.* **2022**, *101*, 1–56. [[CrossRef](#)]
61. Licciardello, G.; Moral, J.; Strano, M.C.; Caruso, P.; Sciara, M.; Bella, P.; Sorrentino, G.; Di Silvestro, S. Characterization of *Colletotrichum* Strains Associated with Olive Anthracnose in Sicily. *Phytopathol. Mediterr.* **2022**, *61*, 139–151. [[CrossRef](#)]
62. López-Moral, A.; Raya-Ortega, M.C.; Agustí-Brisach, C.; Roca, L.F.; Lovera, M.; Luque, F.; Arquero, O.; Trapero, A. Morphological, Pathogenic, and Molecular Characterization of *Colletotrichum acutatum* Isolates Causing Almond Anthracnose in Spain. *Plant Dis.* **2017**, *101*, 2034–2045. [[CrossRef](#)]
63. Materatski, P.; Varanda, C.; Carvalho, T.; Dias, A.B.; Campos, M.D.; Rei, F.; Félix, M.R. Diversity of *Colletotrichum* Species Associated with Olive Anthracnose and New Perspectives on Controlling the Disease in Portugal. *Agronomy* **2018**, *8*, 301. [[CrossRef](#)]
64. Filoda, P.F.; Arellano, A.D.V.; Dallagnol, L.J.; Chaves, F.C. *Colletotrichum acutatum* and *Colletotrichum nymphaeae* Causing Blossom Blight and Fruit Anthracnose on Olives in Southern Brazil. *Eur. J. Plant Pathol.* **2021**, *161*, 993–998. [[CrossRef](#)]
65. Talhinhos, P.; Baroncelli, R. *Colletotrichum* Species and Complexes: Geographic Distribution, Host Range and Conservation Status. *Fungal Divers.* **2021**, *110*, 109–198. [[CrossRef](#)]
66. López-Moral, A.; Agustí-Brisach, C.; Lovera, M.; Arquero, O.; Trapero, A. Almond Anthracnose: Current Knowledge and Future Perspectives. *Plants* **2020**, *9*, 945. [[CrossRef](#)]
67. Shivas, R.G.; Tan, Y.P.; Edwards, J.; Dinh, Q.; Maxwell, A.; Andjic, V.; Liberato, J.R.; Anderson, C.; Beasley, D.R.; Bransgrove, K.; et al. *Colletotrichum* Species in Australia. *Australas. Plant Pathol.* **2016**, *45*, 447–464. [[CrossRef](#)]
68. Chattaoui, M.; Raya, M.C.; Bouri, M.; Moral, J.; Perez-Rodriguez, M.; Trapero, A.; Msallem, M.; Rhouma, A. Characterization of a *Colletotrichum* Population Causing Anthracnose Disease on Olive in Northern Tunisia. *J. Appl. Microbiol.* **2016**, *120*, 1368–1381. [[CrossRef](#)] [[PubMed](#)]
69. Cara, M.; Iliadi, M.K.; Lagogianni, C.S.; Paplomatas, E.J.; Merkuri, J.; Tsitsigiannis, D.I. First Report of *Colletotrichum acutatum* Causing Anthracnose on Olives in Albania. *Plant Dis.* **2021**, *105*, 495. [[CrossRef](#)] [[PubMed](#)]
70. Iliadi, M.K.; Tjamos, E.C.; Antoniou, P.P.; Tsitsigiannis, D.I. First Report of *Colletotrichum acutatum* Causing Anthracnose on Olives in Greece. *Plant Dis.* **2018**, *102*, 820. [[CrossRef](#)]
71. Nawaz, H.H.; Manzoor, A.; Iqbal, M.Z.; Ansar, M.R.; Ali, M.; Muhammad Kakar, K.; Ali Awan, A.; Weiguo, M. *Colletotrichum acutatum*: Causal Agent of Olive Anthracnose Isolation, Characterization, and Fungicide Susceptibility Screening in Punjab, Pakistan. *Plant Dis.* **2023**, *107*, 1329–1342. [[CrossRef](#)] [[PubMed](#)]
72. Riolo, M.; Cacciola, S.O. First Report of *Colletotrichum fioriniae* Associated with Olive Anthracnose in Italy. *J. Plant Pathol.* **2022**, *105*, 363. [[CrossRef](#)]
73. Liu, F.; Damm, U.; Cai, L.; Crous, P.W. Species of the *Colletotrichum gloeosporioides* Complex Associated with Anthracnose Diseases of Proteaceae. *Fungal Divers.* **2013**, *61*, 89–105. [[CrossRef](#)]
74. EFSA PLH Panel (EFSA Panel on Plant Health); Bragard, C.; Baptista, P.; Chatzivassiliou, E.; Di Serio, F.; Gonthier, P.; Jaques Miret, J.A.; Justesen, A.F.; MacLeod, A.; Magnusson, C.S.; et al. Pest Categorisation of *Colletotrichum aenigma*, *C. alienum*, *C. perseae*, *C. siamense* and *C. theobromicola*. *EFSA J.* **2022**, *20*, e07529. [[CrossRef](#)]

Disclaimer/Publisher’s Note: The statements, opinions and data contained in all publications are solely those of the individual author(s) and contributor(s) and not of MDPI and/or the editor(s). MDPI and/or the editor(s) disclaim responsibility for any injury to people or property resulting from any ideas, methods, instructions or products referred to in the content.